Statistical Analysis

The 2-way repeated measures ANOVA was used to compare the groups for changes in lipid profiles and glucose metabolism parameters from baseline to each assessment time. The unpaired t-test adjusted by Holm's method was used for intergroup comparison to avoid multiplicity at multiple time points. A log-rank test was used to compare intensification of DM treatment between the groups.

Results

A total of 1,049 patients were enrolled and randomized to the rosuvastatin or atorvastatin group from March to September 2012 at 132 institutions in Japan; 514 patients in the rosuvastatin group and 504 patients in the atorvastatin group were included in the full analysis set. There were no significant differences between the groups at baseline (**Table S1**).

Lipid Profiles and Glucose Levels

Non-HDL-C showed a significant reduction in both groups (−32.86% in the rosuvastatin group and −31.01% in the atorvastatin group at 12 months) without a significant difference between groups (**Figure 1A**). Low-density lipoprotein cholesterol levels were also decreased at 12 months: −34.79% in the rosuvastatin group and −32.78% in the atorvastatin group (**Figure S1**).

The changes in HbA1c were 0.11 in the rosuvastatin group and 0.12 in the atorvastatin group (**Figure 1B**). There was a significant difference at 6 months even after adjustment for multiple comparisons, but not significant difference between groups throughout the study period. Other glucose metabolism parameters did not show significant differences between groups (**Figure S2**). The cumulative incidence of intensification of DM treatment is shown in **Figure 2**. During the study period, 45 subjects in the rosuvastatin group and 64 subjects in the atorvastatin group were treated with increased DM therapy (**Table S2**). The hazard ratio was 1.46 (95% confidence interval 1.00–2.14) (**Figure 2**).

Safety

Adverse effects occurred in 4.5% of the rosuvastatin group and 5.9% of the atorvastatin group. There were no cases of rhabdomyolysis or of liver function enzyme elevation greater than 3-fold the upper limit of normal.

Discussion

There were no significant changes in non-HDL-C or HbA1c in either group. However, there were difference in the effects on glucose levels and treatment decisions for DM. A meta-analysis has shown that statin therapy is associated with an increased risk of developing DM, but did not show any obvious differences among the individual statins,[9] which are classified as hydrophilic or lipophilic. Takaguri et al reported that lipophilic but not hydrophilic statins significantly affected glucose uptake by adipocytes,[14] and MUSASHI-AMI showed that cardiovascular events tended to be fewer with hydrophilic statins.[15]

To complement the results from previous studies, our results should be interpreted that the choice of statin be considered not only on the basis of potency of cholesterol-lowering effect but also glucose metabolism. In our study results, rosuvastatin and atorvastatin showed different patterns of change in HbA1c. The atorvastatin group tended to be changed to more intensive DM therapy. At 6 months, HbA1c levels showed a statistically significant difference between groups, and that would have influenced physicians' behavior to change the intensity of DM treatment. Consequently, the overall change in HbA1c did not reach statistically significant difference. However, our results suggested rosuvastatin might be preferable to atorvastatin in this study population.

There are several limitations to this study. Firstly, we compared laboratory data mainly as the outcome; in addition, the long-term outcome is uncertain. Moreover, the differences in glucose levels between the 2 statins were determined by the changes in HbA1c levels, in addition to the treatment intensity for DM. Secondly, our study used small dosages based on the Japanese regulation, so the results might underestimate the effects of statins. Besides, this was an open-label study in which the possibility of bias cannot be entirely denied. However, both groups were treated aggressively for DM, as the results for HbA1c level at 12 months were similar between groups, although they were different at 6 months. We believe our findings would be close to the real clinical setting.

Conclusions

Rosuvastatin 5 mg and atorvastatin 10 mg have a similar lowering on non-HDL-C, but might be different in terms of adverse effect on glucose levels.

Funding Sources

LISTEN was funded by the investigator-sponsored study program of AstraZeneca.

Disclosures

H.O. has received grants from the Japan Heart Foundation, and has received research supports or honoraria or both from Astellas Pharma Inc, AstraZeneca KK, Bayer Yakuhin, Ltd, Boehringer Ingelheim Japan, Inc, Bristol-Myers Squibb Company, Chugai Pharmaceutical Co, Ltd, Daiichi Sankyo Company, Limited, Dainippon Sumitomo Pharma Co, Ltd, Kowa Company, Ltd, MSD KK, Novartis Pharma KK, Otsuka Pharmaceutical Co, Ltd, Pfizer Japan Inc, Sanofi KK, and Takeda Pharmaceutical Company Limited.

Y.S. is an adviser at Ono Pharmaceutical Co, Ltd. Y.S. has a clinical commission for an advisor from Ono Pharmaceutical Co, Ltd. Y.S. has received research supports or honoraria or both from Astellas Pharma Inc, AstraZeneca KK, Daiichi Sankyo Company, Limited, Kyowa Hakko Kirin Co, Ltd, Mitsubishi Tanabe Pharma Corporation, MSD KK, Novartis Pharma KK, Otsuka Pharmaceutical Co, Ltd, Pfizer Japan Inc, Shionogi & Co, Ltd, St. Jude Medical Japan Co, Ltd, and Takeda Pharmaceutical Company Limited. Y.S. has endowed departments by MSD Co, Ltd.

M.Y. has received research supports or honoraria or both from Astellas Pharma Inc, Boehringer Ingelheim Japan, Inc, Bristol-Myers Squibb Company, Daiichi Sankyo Company, Limited, Dainippon Sumitomo Pharma Co, Ltd, Eisai Co, Ltd, GlaxoSmithKline KK, Kissei Pharmaceutical Co, Ltd, Kyowa Hakko Kirin Co, Ltd, Mochida Pharmaceutical Co, Ltd, MSD KK, Otsuka Pharmaceutical Co, Ltd, Pfizer Japan Inc, Sanofi KK, and Teijn Pharma Limited.

H.W. has received research supports or honoraria or both from Astellas Pharma Inc, AstraZeneca KK, Boehringer Ingelheim Japan, Inc, Bristol-Myers Squibb Company, Daiichi Sankyo Company, Limited, Dainippon Sumitomo Pharma Co, Ltd, Eli Lilly Japan KK, Johnson & Johnson KK, Kissei Pharmaceutical Co, Ltd, Kowa Company, Ltd, Kyowa Hakko Kirin Co, Ltd, Mitsubishi Tanabe Pharma Corporation, Mochida Pharmaceutical Co, Ltd, MSD KK, Novartis Pharma KK, Novo Nordisk Pharma Ltd, Ono Pharmaceutical Co, Ltd, Pfizer Japan Inc, Sanofi KK, Sanwa Kagaku Kenkyusho Co, Ltd, and Takeda Pharmaceutical Company Limited.

References

1. Miyauchi K, Daida H, Morimoto T, Hiro T, Kimura T, Nakagawa Y, et al. Reverse vessel remodeling but not coronary plaque regression could predict future cardiovascular events in ACS patients with intensive statin therapy: The extended JAPAN-ACS study. *Circ J* 2012; **76:** 825–832.
2. Natsuaki M, Furukawa Y, Morimoto T, Nakagawa Y, Ono K, Kaburagi S, et al. Intensity of statin therapy, achieved low-density lipoprotein cholesterol levels and cardiovascular outcomes in Japanese patients after coronary revascularization: Perspectives from the

CREDO-Kyoto registry cohort-2. *Circ J* 2012; **76:** 1369–1379.
3. Collins R, Armitage J, Parish S, Sleigh P, Peto R; Heart Protection Study Collaborative Group. MRC/BHF Heart Protection Study of cholesterol-lowering with simvastatin in 5963 people with diabetes: A randomised placebo-controlled trial. *Lancet* 2003; **361:** 2005–2016.
4. Colhoun HM, Betteridge DJ, Durrington PN, Hitman GA, Neil HA, Livingstone SJ, et al. Primary prevention of cardiovascular disease with atorvastatin in type 2 diabetes in the Collaborative Atorvastatin Diabetes Study (CARDS): Multicentre randomised placebo-controlled trial. *Lancet* 2004; **364:** 685–696.
5. Knopp RH, d'Emden M, Smilde JG, Pocock SJ. Efficacy and safety of atorvastatin in the prevention of cardiovascular end points in subjects with type 2 diabetes: The Atorvastatin Study for Prevention of Coronary Heart Disease Endpoints in non-insulin-dependent diabetes mellitus (ASPEN). *Diabetes Care* 2006; **29:** 1478–1485.
6. Ridker PM, Danielson E, Fonseca FA, Genest J, Gotto AM Jr, Kastelein JJ, et al. Rosuvastatin to prevent vascular events in men and women with elevated C-reactive protein. *N Engl J Med* 2008; **359:** 2195–2207.
7. Carter AA, Gomes T, Camacho X, Juurlink DN, Shah BR, Mamdani MM. Risk of incident diabetes among patients treated with statins: Population based study. *BMJ* 2013; **346:** f2610.
8. Preiss D, Seshasai SR, Welsh P, Murphy SA, Ho JE, Waters DD, et al. Risk of incident diabetes with intensive-dose compared with moderate-dose statin therapy: A meta-analysis. *JAMA* 2011; **305:** 2556–2564.
9. Sattar N, Preiss D, Murray HM, Welsh P, Buckley BM, de Craen AJ, et al. Statins and risk of incident diabetes: A collaborative meta-analysis of randomised statin trials. *Lancet* 2010; **375:** 735–742.
10. Dormuth CR, Filion KB, Paterson JM, James MT, Teare GF, Raymond CB, et al. Higher potency statins and the risk of new diabetes: Multicentre, observational study of administrative databases. *BMJ* 2014; **348:** g3244.
11. Ridker PM, Pradhan A, MacFadyen JG, Libby P, Glynn RJ. Cardiovascular benefits and diabetes risks of statin therapy in primary prevention: An analysis from the JUPITER trial. *Lancet* 2012; **380:** 565–571.
12. Stone NJ, Robinson JG, Lichtenstein AH, Bairey Merz CN, Blum CB, Eckel RH, et al. 2013 ACC/AHA Guideline on the Treatment of Blood Cholesterol to Reduce Atherosclerotic Cardiovascular Risk in Adults: A report of the American College of Cardiology/American Heart Association Task Force on Practice Guidelines. *Circulation* 2014; **129**(Suppl 2): S1–S45.
13. Rydén L, Standl E, Bartnik M, Van den Berghe G, Betteridge J, de Boer MJ, et al. Guidelines on diabetes, pre-diabetes, and cardiovascular diseases: Executive summary: The Task Force on Diabetes and Cardiovascular Diseases of the European Society of Cardiology (ESC) and of the European Association for the Study of Diabetes (EASD). *Eur Heart J* 2007; **28:** 88–136.
14. Takaguri A, Satoh K, Itagaki M, Tokumitsu Y, Ichihara K. Effects of atorvastatin and pravastatin on signal transduction related to glucose uptake in 3T3L1 adipocytes. *J Pharmacol Sci* 2008; **107:** 80–89.
15. Sakamoto T, Kojima S, Ogawa H, Shimomura H, Kimura K, Ogata Y, et al. Usefulness of hydrophilic vs lipophilic statins after acute myocardial infarction: Subanalysis of MUSASHI-AMI. *Circ J* 2007; **71:** 1348–1353.

Appendix

LISTEN Investigators

Hisao Mori, Takao Nagasu, Kazuo Maeda, Kumio Iroden, Kazuaki Uchiyama, Toshibumi Hogi, Fumiaki Ono, Hideki Kikuchi, Masahiko Kuroda, Eiichi Tokutake, Tsutomu Hayashi, Keiichi Chin, Hareaki Yamamoto, Yoshihisa Takada, Nobuaki Oka, Masako Waki, Shuji Kagawa, Masaru Murakami, Toshihiro Arizumi, Hifumi Atsuko, Akira Maki, Hiroo Miyagi, Kentarou Yata, Shinsuke Takei, Masami Kogure, Masayuki Nakano, Youichi Ehara, Akira Ota, Hideo Ayame, Masahiro Sugawara, Tetsuo Munakata, Koichi Hasegawa, Shoshi Matsuda, Takashi Fujimoto, Shinichi Matsumoto, Osame Tanaka, Akira Soejima, Tomoyuki Shibuya, Soichi Honda, Shuji Mizumachi, Yutaka Wakasa, Hirokuni Etsuda, Toshifumi Matsuno, Tetsuya Tsurumachi, Nobushige Ote, Hisataka Tegoshi, Masaki Matsuoka, Kengo Matsumoto, Nobuyuki Enomoto, Masayuki Yanagi, Katsumi Yoshida, Koji Oida, Masahiro Fukuda, Koji Takaki, Tomohiro Katsuya, Takuma Eto, Hiroki Kamata, Kohsuke Minamisawa, Hiroaki Seino, Ichitaro Takada, Hideto Ishii, Yoshiko Kubota, Hidetaka Kanazawa, Shinya Hiramitsu, Yoshihiro Fujii, Yuichiro Nakamura, Yasuhiro Hashiguchi, Shinya Okamoto, Kazuo Ikeda, Hiroshi Nishimura, Takahiko Kawagishi, Kazuya Shigenobu, Masaaki Arima, Kenichi Yamamoto, Yasushi Suzuki, Naomi Yoshimura, Takahiro Hayashi, Satoru Hasegawa, Doniwa Ken-ichi, Masatoshi Yanagisawa, Toshiki Tatsumura, Kimikazu Sawai, Hiroto Moriyasu, Masaru Matsuda, Shuichi Kawano, Kazuo Sakabe, Akiyo Shinoda, Ken Takenaka, Ichiro Kanamori, Toshiyuki Kashiwagi, Arata Iwasaki, Naoto Yokota, Kou Arakawa, Masanori Inoue, Masahiro Ueno, Yuji Nakatani, Takayuki Higashi, Kiyohito Takahashi, Shuichi Matsuo, Yoshiyuki Ishii, Shoichi Kitano, Hiroshi Tanaka, Hideaki Jinnouchi, Naotaka Kusunose, Toshimitsu Jikuhara, Hiroshi Kobayashi, Yasuhiko Kawade, Naoki Kawai, Junpei Iinuma, Kuniyuki Takai, Takao Yasue, Tsuguo Niimi, Yukinori Kawase, Reiki Yoshida, Koji Ishimura, Hatsumi Masaki, Joji Koike, Naoto Ishikawa, Jun Arao, Toru Kinugawa, Haruyoshi Nakao, Mikio Yamaguchi, Shinichiro Otake, Michio Tamatani, Yumiko Ide, Haruyuki Taguchi, Nobuyuki Azuma, Izuru Masuda, Harunori Oda, Kazuhiko Takano, Ren Horibe, Junichiro Kondo.

Supplementary Files

Supplementary File 1

Table S1. Baseline characteristics of subjects in the LISTEN Study

Table S2. Change in therapy for DM among subjects of the LISTEN Study

Figure S1. The changes of LDL-C (low-density lipoprotein cholesterol), TC (total-cholesterol), HDL-C (high-density lipoprotein cholesterol), TG (triglyceride). Analyses performed using repeated measures ANOVA for overall comparison between treatment groups.

Figure S2. The changes of Blood glucose, Insulin and 1,5-AG. Analyses performed using repeated measures ANOVA for overall comparison between treatment groups.

Please find supplementary file(s);
http://dx.doi.org/10.1253/circj.CJ-14-0810

Am J Physiol Heart Circ Physiol 307: H1626–H1633, 2014.
First published October 3, 2014; doi:10.1152/ajpheart.00228.2014.

Hydrogen gas attenuates embryonic gene expression and prevents left ventricular remodeling induced by intermittent hypoxia in cardiomyopathic hamsters

Ryuji Kato,[1] Atsuo Nomura,[1] Aiji Sakamoto,[2] Yuki Yasuda,[1] Koyuha Amatani,[1] Sayuri Nagai,[1] Yoko Sen,[1] Yoshio Ijiri,[1] Yoshikatsu Okada,[3] Takehiro Yamaguchi,[4] Yasukatsu Izumi,[5] Minoru Yoshiyama,[4] Kazuhiko Tanaka,[1] and Tetsuya Hayashi[1]

[1]*Laboratory of Cardiovascular Pharmacotherapy and Toxicology, Osaka University of Pharmaceutical Sciences, Takatsuki, Japan;* [2]*Laboratory of Vascular Biology, National Cerebral and Cardiovascular Center, Suita, Japan;* [3]*Department of Pathology, Osaka Medical College, Daigakumachi, Takatsuki, Japan;* [4]*Department of Cardiovascular Medicine, Osaka City University Graduate School of Medicine, Osaka, Japan; and* [5]*Department of Pharmacology, Osaka City University Graduate School of Medicine, Osaka, Japan*

Submitted 4 April 2014; accepted in final form 23 September 2014

Kato R, Nomura A, Sakamoto A, Yasuda Y, Amatani K, Nagai S, Sen Y, Ijiri Y, Okada Y, Yamaguchi T, Izumi Y, Yoshiyama M, Tanaka K, Hayashi T. Hydrogen gas attenuates embryonic gene expression and prevents left ventricular remodeling induced by intermittent hypoxia in cardiomyopathic hamsters. *Am J Physiol Heart Circ Physiol* 307: H1626–H1633, 2014. First published October 3, 2014; doi:10.1152/ajpheart.00228.2014.—The prevalence of sleep apnea is very high in patients with heart failure (HF). The aims of this study were to investigate the influence of intermittent hypoxia (IH) on the failing heart and to evaluate the antioxidant effect of hydrogen gas. Normal male Syrian hamsters (n = 22) and cardiomyopathic (CM) hamsters (n = 33) were exposed to IH (repeated cycles of 1.5 min of 5% oxygen and 5 min of 21% oxygen for 8 h during the daytime) or normoxia for 14 days. Hydrogen gas (3.05 vol/100 vol) was inhaled by some CM hamsters during hypoxia. IH increased the ratio of early diastolic mitral inflow velocity to mitral annulus velocity (E/e′, 21.8 vs. 16.9) but did not affect the LV ejection fraction (EF) in normal Syrian hamsters. However, IH increased E/e′ (29.4 vs. 21.5) and significantly decreased the EF (37.2 vs. 47.2%) in CM hamsters. IH also increased the cardiomyocyte cross-sectional area (672 vs. 443 μm^2) and interstitial fibrosis (29.9 vs. 9.6%), along with elevation of oxidative stress and superoxide production in the left ventricular (LV) myocardium. Furthermore, IH significantly increased the expression of brain natriuretic peptide, β-myosin heavy chain, c-*fos*, and c-*jun* mRNA in CM hamsters. Hydrogen gas inhalation significantly decreased both oxidative stress and embryonic gene expression, thus preserving cardiac function in CM hamsters. In conclusion, IH accelerated LV remodeling in CM hamsters, at least partly by increasing oxidative stress in the failing heart. These findings might explain the poor prognosis of patients with HF and sleep apnea.

heart failure; intermittent hypoxia; oxidative stress; cardiomyopathic hamster; hydrogen gas

SLEEP APNEA SYNDROME (SAS) is a breathing disorder characterized by recurrent episodes of apnea and/or hypopnea that increases the risk of cardiovascular morbidity and mortality (10, 19, 26). In persons with SAS, recurrent hypopnea/apnea leads to intermittent hypoxia (IH). The prevalence of SAS is much higher in patients with established cardiovascular disease, and central sleep apnea is associated with the more severe forms of heart failure (17), although the mechanisms underlying periodic breathing in patients with heart failure (HF) are complex and multifactorial.

Oxidative stress arises because of an imbalance between free radical production and endogenous antioxidant defenses and is increased in patients with HF (4). Free radicals have also been linked to endothelial dysfunction and increased sympathetic tone (2, 16), whereas intravenous infusion of antioxidants reduces free radical levels and attenuates sympathetic activity in animal models of HF (32). It has been suggested that hydrogen gas produced in the large intestine by intestinal bacteria might scavenge hydroxyl radicals (6), and it was recently reported that hydrogen gas selectively scavenges hydroxyl radicals and exerts an antioxidant effect (23). We previously reported that inhalation of hydrogen gas could prevent dyslipidemia and could also suppress oxidative stress in the left ventricular (LV) myocardium of mice exposed to IH (13). Accordingly, we considered that hydrogen gas might exert a cardioprotective effect in cardiomyopathic (CM) hamsters.

Because the effects of IH on cardiovascular disease have not been clarified, we performed the present study to examine the influence of IH on the heart in CM hamsters (an animal model of human hereditary cardiomyopathy) and to evaluate the antioxidant effect of hydrogen gas on the failing heart during exposure to IH.

MATERIALS AND METHODS

Animals. Normal Syrian hamsters (aged 24 wk, n = 22) were obtained from Japan SLC (Hamamatsu, Shizuoka, Japan). By crossing BIO14.6 hamsters (Bio Breeders, Fitchburg, MA) and Syrian hamsters, we generated CM hamsters (aged 20–24 wk, n = 33) with homozygous deletion for the δ-sarcoglycan gene (28). The hamsters were housed at a temperature of 24 ± 1°C and a humidity of 55 ± 10%, with lights on from 6:00 to 18:00 and free access to tap water and solid feed (NMF, Oriental Yeast, Tokyo, Japan). The Osaka University of Pharmaceutical Sciences Experimental Animal Research Committee approved the study protocol and the animal care methods. All experiments were conducted in accordance with the National Institutes of Health guidelines for the care and use of laboratory animals.

Study protocol. Hamsters were placed in a chamber and exposed to IH (repeated cycles of 1.5 min of 5% oxygen and 5 min of 21%

Address for reprint requests and other correspondence: T. Hayashi, Laboratory of Cardiovascular Pharmacotherapy and Toxicology, Osaka Univ. of Pharmaceutical Sciences, 4-20-1 Nasahara, Takatsuki, Osaka 569-1094, Japan (e-mail: hayashi@gly.oups.ac.jp).

Table 1. *Body weight, heart weight, and heart weight/body weight ratio*

Group	BW, g	HW, mg	HW/BW ratio, mg/g
Syrian normoxia	148 ± 4.50	0.418 ± 0.015	2.84 ± 0.114
Syrian hypoxia	149 ± 6.79	0.457 ± 0.018	3.08 ± 0.093
CM normoxia	134 ± 7.07	0.495 ± 0.023	3.74 ± 0.167*
CM hypoxia	131 ± 5.58	0.560 ± 0.029*	4.29 ± 0.217**,††
CM hypoxia + H_2	143 ± 7.92	0.504 ± 0.023	3.57 ± 0.185

CM, cardiomyopathy; BW, body weight; HW, heart weight. Data are shown as means ± SE (n = 5–13). *P < 0.05 compared with the Syrian normoxia group; **P < 0.01 compared with the Syrian normoxia group; ††P < 0.01 compared with the Syrian hypoxia group.

oxygen for 8 h during the daytime) for 2 wk with or without inhalation of hydrogen gas (3.05 vol/100 vol) during the hypoxic periods. Hamsters maintained under normoxic conditions in the same room served as controls. Thus we assessed Syrian hamsters housed under normoxic conditions (Syrian normoxia group), Syrian hamsters exposed to IH (Syrian hypoxia group), CM hamsters housed under normoxic conditions (CM normoxia group), CM hamsters exposed to IH (CM hypoxia group), and CM hamsters that inhaled a mixture of N_2/H_2 gas during IH (CM hypoxia + H_2 group). Cardiac function was evaluated by echocardiography under anesthesia induced by intraperitoneal injection of pentobarbital sodium (50 mg/kg) on the day after the last exposure to hypoxia.

Echocardiographic analysis. Transthoracic echocardiography was performed using a Vivid E9 instrument (GE Healthcare, Salt Lake City, UT). In brief, the LV ejection fraction (LVEF) was calculated from the LV end-diastolic volume (LVEDV) and LV end-systolic volume (LVESV) obtained using a modified Simpson's method (34). In addition, pulsed-wave Doppler spectra [early LV filling velocity (E wave) and late LV filling velocity due to atrial contraction (A wave)] of mitral inflow were recorded in the apical four-chamber view with the sample volume being placed near the tips of the mitral leaflets at the position where velocity was maximal and flow was laminar. The ratio of E wave velocity to A wave velocity (E/A ratio) was then calculated. Furthermore, the early velocity (e′) and late velocity (a′) of the mitral annulus were determined by tissue Doppler imaging, and the ratio of E to e′ (E/e′ ratio) was calculated.

Histological assessment. Hearts (some arrested in diastole with saturated potassium chloride) were excised and transected below the mitral valve, after which the upper half was examined by light microscopy. The LV free wall myocardium was excised for assessment by electron microscopy, immunohistochemistry, and real-time reverse transcription-polymerase chain reaction (RT-PCR) analysis. For light microscopy, cardiac tissues were fixed in 10% formaldehyde, embedded in paraffin, and cut into 4-μm sections. Photographs were taken with an ECLIPSE 80i light microscope (Nikon, Tokyo, Japan) at a magnification of ×4 and were transformed into binary images, and the cardiac cross-sectional area was evaluated at a magnification of ×400 by the method previously reported (8) using ImageJ version 1.44 software (National Institutes of Health, Bethesda, MD). Briefly, in nucleated transverse sections stained with hematoxylin-eosin, cardiomyocytes with both a clear nucleus and intact cellular membrane were measured using NIS-Elements version 3.07 software (Nikon), and at least 30 cardiomyocytes were analyzed per heart. After staining with Sirius red, color images were randomly selected from five high-power fields (at a magnification of ×200), and the collagen volume ratio (%) was calculated as described elsewhere (33). The LV free wall myocardium was fixed in 4% paraformaldehyde containing 0.25% glutaraldehyde and 4.5% sucrose. Ultrathin sections were cut from the fixed blocks, stained with uranyl acetate and lead citrate, and examined using a Hitachi model H-7650 electron microscope (Hitachi, Tokyo, Japan) (12).

Terminal deoxynucleotidyl transferase-mediated dUTP-biotin end labeling. LV myocardial tissue samples were assessed by terminal deoxynucleotidyl transferase-mediated dUTP-biotin nick end labeling (TUNEL) using Apop Tag peroxidase in situ apoptosis detection kits (Millipore Japan, Tokyo, Japan). Negative controls were processed with distilled water, and endometrium was used as the positive control. After cells were counterstained with Mayer's hematoxylin, TUNEL-positive cells were counted as described elsewhere (15).

Immunohistochemistry of 4-hydroxy-2-nonenal expression. The amount of 4-hydroxy-2-nonenal (4-HNE)-modified protein adducts in paraffin sections of the left ventricle was determined by immunohistochemical staining. Sections were incubated with a monoclonal antibody for 4-HNE (Japan Institute for the Control of Aging, Shizuoka, Japan) and with a secondary antibody (biotinylated anti-mouse IgG), followed by incubation with Vectastain Elite ABC reagent (Vector, Burlingame, CA). The area of 4-HNE staining was then compared with the mean area on control sections (defined as 1.0).

Detection of superoxide in LV myocardium. Freshly frozen unfixed LV myocardial specimens were incubated with 10 μmol/l of dihydroethidium (DHE) (Molecular Probes, Eugene, OR) for 30 min in a light-protected humidified chamber at 37°C. Sections were examined using a BZ-8000 fluorescence microscope (KEYENCE, Osaka, Japan), and the fluorescence intensity of DHE was quantified using NIH Image 1.61 software and compared with the mean control intensity to detect in situ superoxide production.

Quantitative real-time RT-PCR. Total RNA was extracted from LV and RV myocardial tissues using TRI reagent (Molecular Research Center, Cincinnati, OH). Complementary DNA was synthesized from total RNA by reverse transcription using a Transcriptor Universal cDNA Master kit (Roche Diagnostics, Basel, Switzerland). The primers and probes were designed for the nucleotide sequence of hamster brain natriuretic peptide (BNP), β-myosin heavy chain (β-MHC), c-*fos*, c-*jun*, and glyceraldehyde-3-phosphate dehydrogenase (GAPDH) using Probefinder v. 2.45 software (http://qpcr.probefinder.com/roche3.html), which specifies a set of specific primers plus the TaqMan locked nucleic acid probe from the Roche Universal Probe Library collection. Universal Probes No. 38 for β-MHC, No. 46 for c-*fos*, No. 78 for c-*jun*, No. 80 for GAPDH, and No. 95 for BNP were purchased from Roche Diagnostics. The mRNA levels were

Table 2. *Echocardiographic findings*

Group	Dd, mm	Ds, mm	E, cm/s	A, cm/s	E/A	e′, cm/s	E/e′	LVEF, %
Syrian normoxia	4.71 ± 0.17	3.15 ± 0.14	84.6 ± 3.13	60.9 ± 6.18	1.43 ± 0.08	5.23 ± 0.44	16.9 ± 1.80	60.2 ± 0.56
Syrian hypoxia	5.07 ± 0.17	3.59 ± 0.15	81.5 ± 5.92	54.8 ± 8.06	1.55 ± 0.13	4.23 ± 0.91	21.8 ± 3.93	61.5 ± 0.76
CM normoxia	5.89 ± 0.39	4.43 ± 0.44	79.5 ± 5.64	49.2 ± 4.72	1.69 ± 0.13	3.84 ± 0.43	21.5 ± 1.70	47.2 ± 3.41*,†
CM hypoxia	6.23 ± 0.36*	4.82 ± 0.50	77.9 ± 5.00	55.3 ± 4.34	1.43 ± 0.05	2.76 ± 0.24**	29.4 ± 2.29**,‡	37.2 ± 3.24**,††,‡
CM hypoxia + H_2	5.17 ± 0.28	3.61 ± 0.17	78.4 ± 4.42	56.7 ± 3.64	1.39 ± 0.03	4.04 ± 0.45	20.0 ± 1.59§	60.9 ± 0.92§§

CM, cardiomyopathy; Dd, left ventricular end-diastolic diameter; Ds, LV end-systolic diameter; E, early rapid filling wave of mitral inflow; A, atrial contraction wave of mitral inflow; e′, early velocity of the mitral annulus; LVEF, left ventricular ejection fraction. Data are shown as means ± SE (n = 5–9). *P < 0.05 compared with the Syrian normoxia group; **P < 0.01 compared with the Syrian normoxia group; †P < 0.05 compared with the Syrian hypoxia group; ††P < 0.01 compared with the Syrian hypoxia group; ‡P < 0.05 compared with the CM normoxia group; §P < 0.05 compared with the CM hypoxia group; §§P < 0.01 compared with the CM hypoxia group.

measured using a LightCycler (Roche Diagnostics) and were normalized by comparison with the level of GAPDH mRNA as the internal control.

Statistical analysis. Values are shown as means ± SE. Data were statistically analyzed by using one-way ANOVA followed by the Tukey-Kramer multiple comparison test, and $P < 0.05$ was considered to indicate a significant difference.

RESULTS

Heart weight and body weight. Heart weight was significantly increased in the CM hypoxia group compared with the Syrian normoxia group. The heart weight-to-body weight ratio was significantly increased in the CM hypoxia group compared with both the Syrian normoxia group and the Syrian hypoxia group (Table 1).

Echocardiographic findings. LVEF was significantly smaller in the CM normoxia group compared with the Syrian normoxia and Syrian hypoxia groups (Table 2). IH led to a significant increase of LV end-diastolic diameter, E/e′, and LVEF in the CM hypoxia group, but not in the Syrian hypoxia group (Table 2 and Fig. 1). In contrast, these changes were less marked in the CM hypoxia + H_2 group, and LVEF showed significant improvement (Table 2 and Fig. 1).

Histological findings. In CM hamsters, exposure to IH induced cardiomegaly and a significant increase of cardiomyocytes cross-sectional area (Fig. 2). The CM hypoxia group showed an increase in degeneration of cardiomyocytes, including myofibrillar lysis, disarray of myofibers, and interstitial fibrosis (Fig. 2, *H* and *I*). Electron microscopy revealed mild myofiber disarray and variation of mitochondrial size in CM hamsters kept under normoxic conditions. Exposure to IH resulted in an increase of myofibrillar lysis, mitochondrial degeneration, dissociation of intercalated discs, and Z-line streaming (Fig. 3). All of these changes induced by IH in CM hamsters were suppressed by inhalation of hydrogen gas (Fig. 2, *K* and *L*, and Fig. 3*F*).

TUNEL findings. The number of TUNEL-positive cells in the LV myocardium was significantly increased in the CM hypoxia group, whereas it was significantly reduced in the CM hypoxia + H_2 group (Fig. 4).

Superoxide production and 4-HNE expression in the LV myocardium. In the CM hypoxia group, superoxide production (detected by DHE labeling) and 4-HNE-modified protein adducts were significantly increased in the LV myocardium, whereas these changes were significantly suppressed in the CM hypoxia + H_2 group (Fig. 5).

Real-time RT-PCR. In the CM hypoxia group, expression of BNP and β-MHC mRNA was significantly increased in the LV myocardium compared with the Syrian normoxia group. Inha-

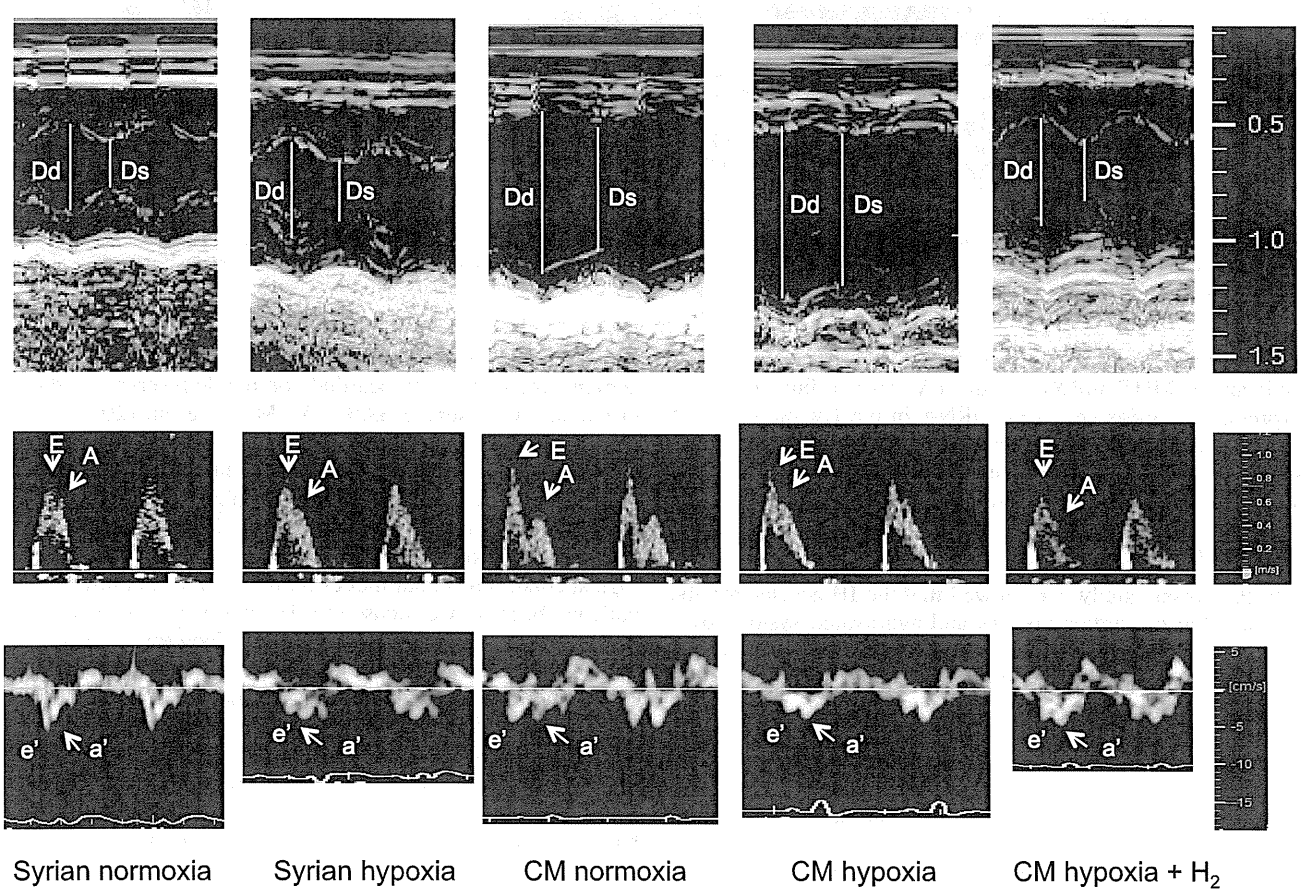

Fig. 1. Echocardiographic findings after 2 wk of intermittent hypoxia. Changes in left ventricular (LV) end-diastolic diameter (D_d), LV end-systolic diameter (D_s), pulsed-wave Doppler parameters [early rapid filling wave (E) and atrial contraction wave (A) of mitral inflow], and tissue Doppler parameters [early (e′) and late (a′) velocities of the mitral annulus]. Note that the quantitative data are summarized in Table 2.

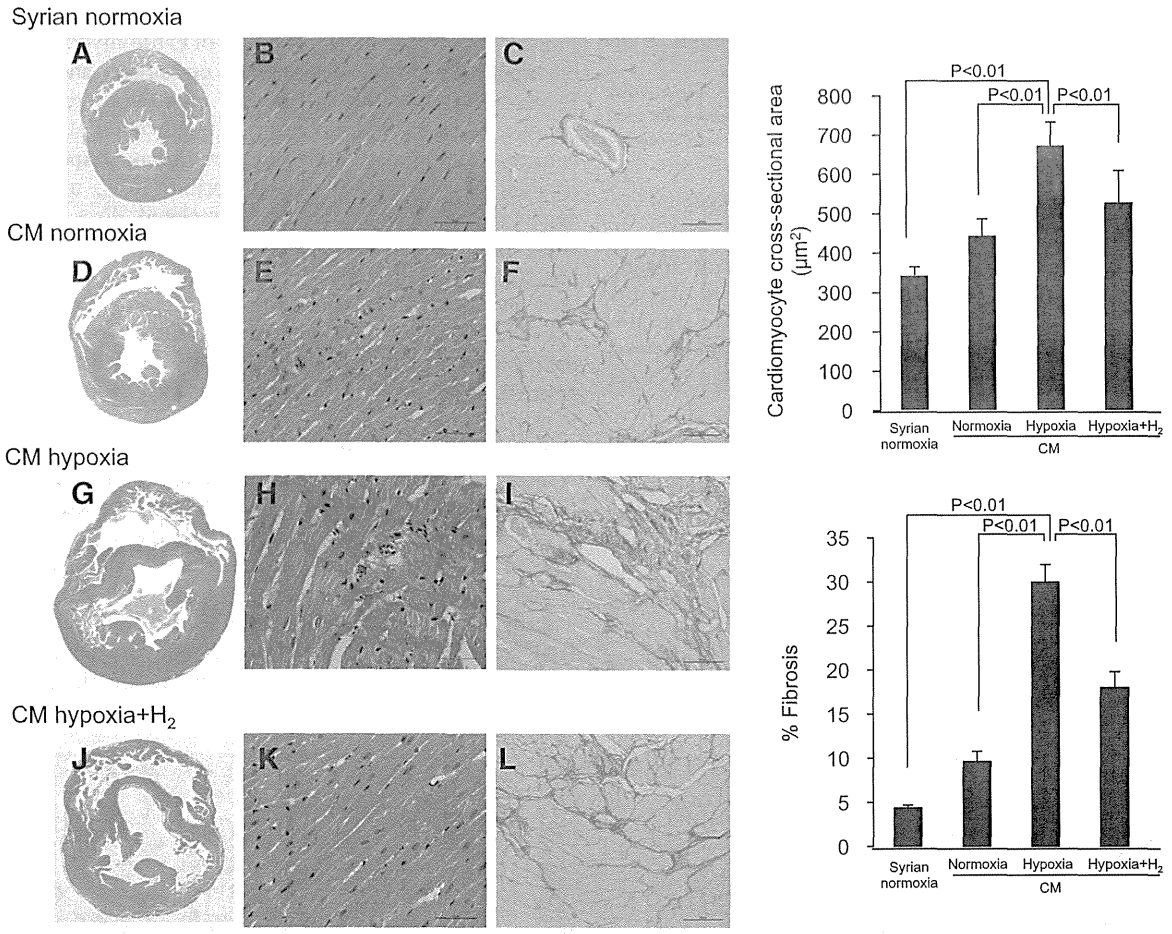

Fig. 2. Representative light micrographs, cardiomyocyte cross-sectional area, and collagen content (%fibrosis) in the LV myocardium of cardiomyopathic (CM) hamsters. Intermittent hypoxia caused cardiac hypertrophy (*G*), cardiomyocyte degeneration (*H*), and increased perivascular fibrosis (*I*). These abnormalities were suppressed by inhalation of hydrogen gas (*J–L*). Intermittent hypoxia significantly increased the cardiomyocyte cross-sectional area and interstitial fibrosis, whereas inhaling hydrogen gas significantly suppressed these changes. Values are shown as means ± SE (n = 5–16).

lation of hydrogen gas significantly reduced the expression of BNP and β-MHC mRNA in the LV myocardium (Fig. 6). Expression of c-*fos* and c-*jun* mRNA in the LV myocardium was also significantly increased in the CM hypoxia group, whereas inhalation of hydrogen gas significantly reduced myocardial expression of c-*fos* and c-*jun* mRNA (Fig. 6).

DISCUSSION

In the present study, we showed that the IH accelerated the degeneration of cardiomyocytes and aggravated systolic dysfunction in CM hamsters, whereas these deleterious effects of IH were not seen in Syrian hamsters. The CM hypoxia group displayed hypertrophy of cardiomyocytes, as well as increased expression of c-*fos* and c-*jun* mRNA. On the other hand, inhaling a low concentration (3.05 vol/100 vol) of hydrogen gas attenuated cardiomyocyte hypertrophy and perivascular fibrosis in the LV myocardium, resulting in the preservation of cardiac function.

LV diastolic function is frequently impaired in patients with SAS (1, 18). In the present study, exposure to IH for 2 wk mainly caused LV systolic dysfunction in CM hamsters and had a minimal effect on the heart in normal Syrian hamsters. We previously used dobutamine stress echocardiography to demonstrate that the myocardial contractile reserve is reduced in patients with severe SAS (25). Maeda et al. (20) recently reported that a longer duration of IH induces autophagy in the normal rat heart, which maintains contractile function and prevents necrosis. Their differing findings might be due to differences of the animal model and the duration of hypoxic stress. In addition, it should be remembered that the physiological conditions in our model are different from those in SAS patients, because we focused on IH and neglected barometric pressure and acid-base disturbance. Therefore, change of $PaCO_2$ should be taken into consideration in a future study.

In CM hamsters, we found that IH increased cardiac hypertrophy, interstitial fibrosis, and cardiomyocyte degeneration (including mitochondrial destruction and myofibrillar lysis), but these changes did not occur in normal Syrian hamsters. Intriguingly, streaming of Z-lines was often observed in CM hamsters. It has been reported that Z-line degeneration is observed in the myocardium with genetic mutations of dystrophin-associated glycoproteins, including δ-sarcoglycan (31). The myocardium of CM hamsters would be expected to be fragile, and genomic deletion of δ-sarcoglycan might have

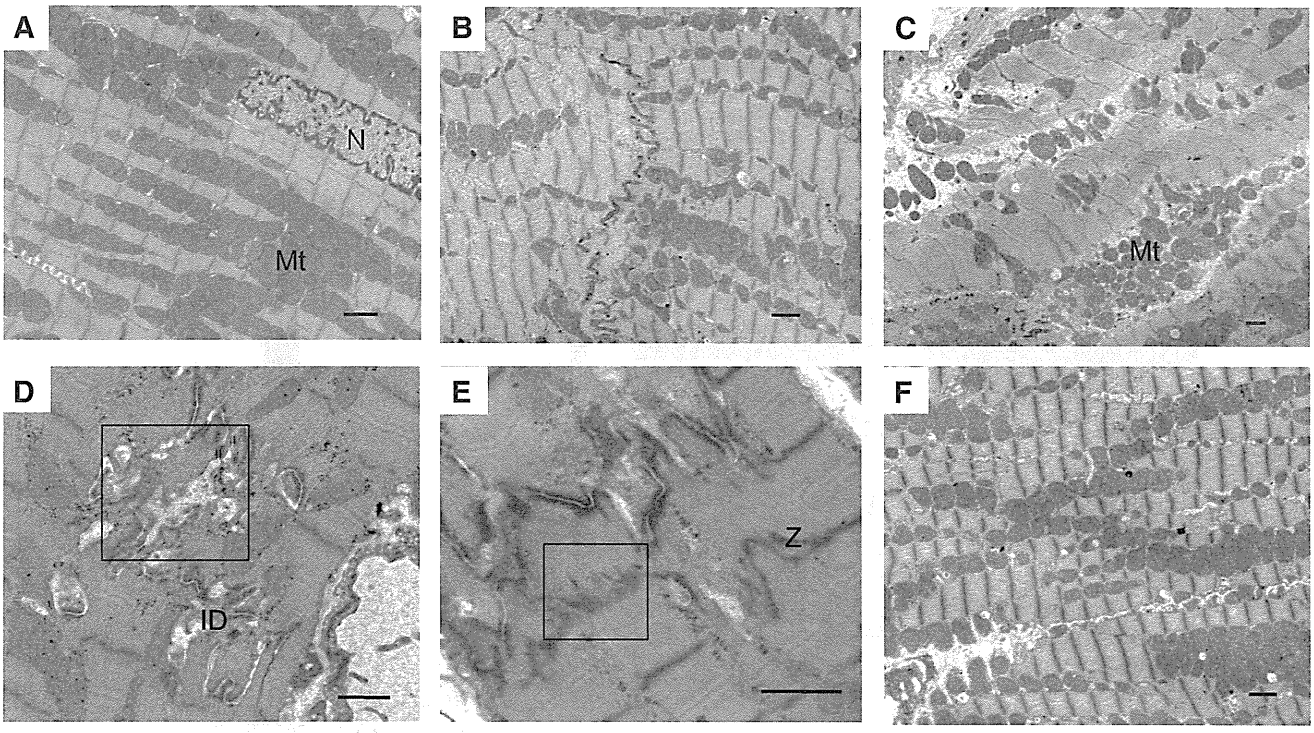

Fig. 3. Electron micrographs of the LV myocardium. A normal Syrian hamster (*A*). Mt, mitochondria; N, nucleus. Mild myofiber disarray and variation of mitochondrial sizes are observed in CM hamster maintained under normoxic conditions (*B*). Intermittent hypoxia (IH) has increased myofibrillar lysis and Mt degeneration in a CM hamster (*C*). Partial dissociation (square) of intercalated disc (ID) (*D*) and Z-line (Z) streaming (square) (*E*) were often observed in the CM hypoxia group. All of the changes seen in CM hamsters due to IH were suppressed by inhaling hydrogen gas (*F*). Scale bar, 1 μm.

been the underlying cause of histological changes that were accelerated by IH in CM hamsters.

Although the precise mechanisms through which SAS aggravates heart failure are unknown, it has been suggested that oxidative stress might play an important role in the progression of cardiovascular disease (27). In the present study, superoxide production and 4-HNE-modified protein adducts were increased in the LV myocardium by IH, suggesting an increase of oxidative stress, and these changes were inhibited by inhaling a low concentration of hydrogen gas. Furthermore, the number of degenerated mitochondria was decreased, and the ultrastructural architecture of the LV myocardium was preserved in the CM hypoxia + H_2 group. It has been reported that H_2 gas selectively scavenges hydroxyl radicals (24). It has also been reported that hydrogen protects cells and tissues against oxidative stress by scavenging hydroxyl radicals (22) and might prevent a decrease of cellular ATP levels (23). Since we found that IH aggravated underlying abnormalities and reduced systolic function, one of the mechanisms through which adaptive servo-ventilation improves congestive HF might be alleviation of oxidative stress (11). We previously evaluated the effect of hydrogen gas inhalation on LV remodeling and dyslipidemia in mice when hydrogen was inhaled during reoxygenation, during hypoxia, or throughout the experimental period (13), and we showed that inhalation during hypoxia reduced oxidative stress and improved systolic dysfunction in the failing heart. Therefore, inhalation of hydrogen gas using adaptive servo-ventilation might be an effective treatment for patients with HF and periodic apnea. In the present study, oxidative stress was evaluated by immunohistochemistry. Our preliminary study demonstrated that malondialdehyde, a biomarker of lipid peroxidation, was significantly increased in LV myocardium after exposure to intermittent hypoxia (data not shown). Additional parameters of oxidative stress like malondialdehyde should be employed in future studies.

Myocardial remodeling is associated with upregulation of the expression of embryonic gene isoforms such as c-*fos* and c-*jun* (5, 21). BNP and β-MHC are well-established markers of cardiomyocyte hypertrophy. In the present study, changes of BNP and β-MHC mRNA expression showed that IH increased cardiac hypertrophy and that it was suppressed by inhaling hydrogen gas. We found that c-*fos* and c-*jun* mRNA expression was significantly increased in the LV myocardium of the CM hypoxia group. Increased c-*fos* and c-*jun* levels might suggest transcriptional activation of activator protein 1 (AP-1) (3), because AP-1 plays a pivotal role in the ERK/JNK signaling pathways and overexpression of c-*jun* and c-*fos* is a common feature of myocardial hypertrophy in rodents (3, 7). In turn, the upregulation of c-*fos* and c-*jun* might accelerate myocardial degeneration. Various stimuli can activate AP-1, including inflammatory cytokines, growth factors, and oxidative stress (9, 14, 30), whereas inhaled hydrogen gas scavenges free radicals and decreases oxidative stress, so that c-*fos* and c-*jun* mRNA expression was decreased by inhalation of hydrogen in the present study. AP-1 has been reported to induce aldose reductase-like gene, which is involved in the biosynthesis of PGF2α. It has been reported that PGF2α inhibits expression of the sarco(endo)plasmic reticulum Ca^{2+}-ATPase 2 (SERCA2)

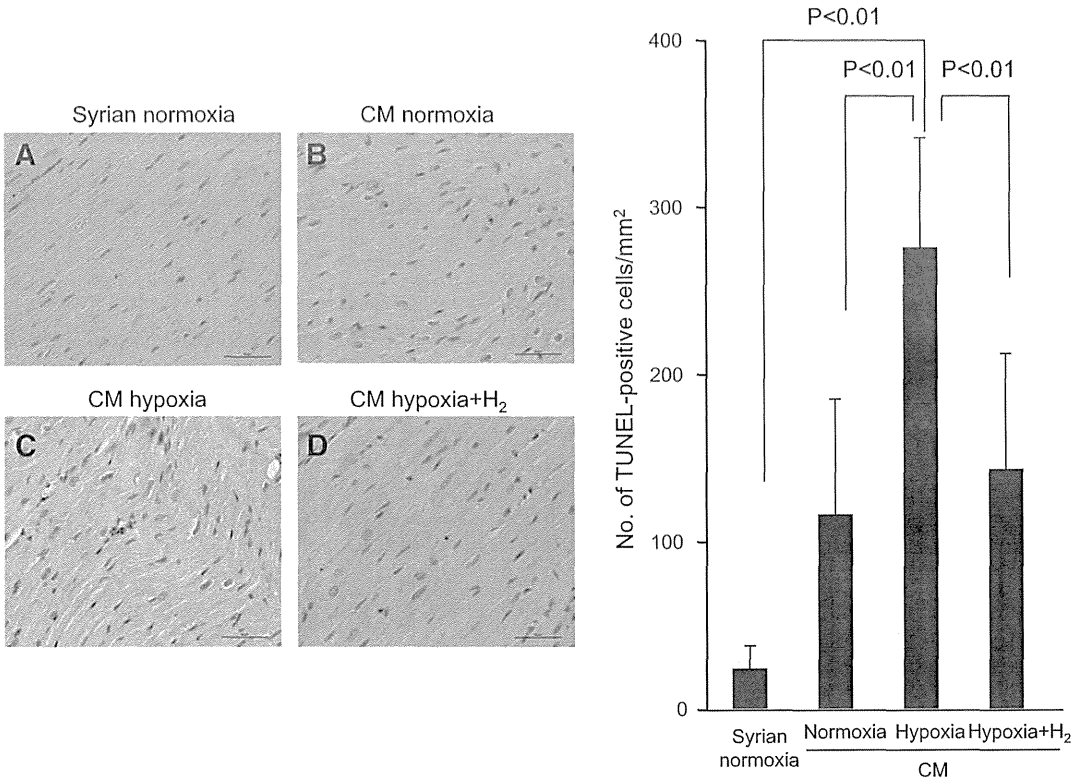

Fig. 4. Terminal deoxynucleotidyl transferase-mediated dUTP nick end labeling (TUNEL) staining of LV myocardium in CM hamsters. Compared with hamsters from the Syrian normoxia group (*A*) and the CM normoxia group (*B*), TUNEL-positive cells are significantly increased in the LV myocardium of a CM hamster exposed to intermittent hypoxia (CM hypoxia group) (*C*), whereas these cells are significantly decreased by inhaling hydrogen gas (CM hypoxia + H_2 group) (*D*). Values are shown as means ± SE (n = 4–7).

gene and thus causes diastolic dysfunction (29). Accordingly, further studies are needed with a focus on the molecular pathways involved in the pathogenesis of cardiomyopathy, including aldose reductase-like gene expression.

In conclusion, exposure of CM hamsters to IH promoted cardiomyocyte degeneration and systolic dysfunction, at least partly through increased oxidative stress, which might explain the poor prognosis of HF patients with SAS. Inhalation of hydrogen gas attenuated the deleterious changes in CM hamsters and might be a novel treatment strategy for HF, especially in patients who also have SAS.

ACKNOWLEDGMENTS

We are grateful to Y. Ogami, C. Ota, and M. Ito for expert technical assistance. We also thank Y. Fujiwara, J. Kawakami, M. Matsui, M. Muroya, S. Tanigawa, M. Unno, and F. Yoshimura for valuable assistance throughout experiments.

GRANTS

This work was supported in part by the Vehicle Racing Commemorative Foundation and by a Grant-in-Aid for Scientific Research from the Japanese Ministry of Education, Culture, Sports, Science and Technology Grant-in-Aid 23590267 (Kakenhi).

DISCLOSURES

No conflicts of interest, financial or otherwise, are declared by the author(s).

AUTHOR CONTRIBUTIONS

R.K., A.N., Y.Y., K.A., S.N., Y.S., T.Y., Y. Izumi, and T.H. performed experiments; R.K., A.N., Y. Ijiri, T.Y., Y. Izumi, and T.H. analyzed data; R.K., A.N., Y. Ijiri, Y.O., Y. Izumi, M.Y., and T.H. interpreted results of experiments; R.K., A.N., Y. Izumi, and T.H. prepared figures; R.K., A.S., and T.H. drafted manuscript; R.K., A.N., A.S., Y.Y., K.A., S.N., Y.S., Y. Ijiri, Y.O., T.Y., Y. Izumi, M.Y., K.T., and T.H. approved final version of manuscript; A.S. and T.H. conception and design of research; A.S., M.Y., K.T., and T.H. edited and revised manuscript.

REFERENCES

1. **Arias MA, García-Río F, Alonso-Fernández A, Mediano O, Martínez I, Villamor J.** Obstructive sleep apnea syndrome affects left ventricular diastolic function: effects of nasal continuous positive airway pressure in men. *Circulation* 112: 375–383, 2005.
2. **Baguet JP, Narkiewicz K, Mallion JM.** Update on hypertension management: obstructive sleep apnea and hypertension. *J Hypertens* 24: 205–208, 2006.
3. **Blanchette J, Abu-Dayyeh I, Hassani K, Whitcombe L, Olivier M.** Regulation of macrophage nitric oxide production by the protein tyrosine phosphatase Src homology 2 domain phosphotyrosine phosphatase 1 (SHP-1). *Immunology* 127: 123–133, 2009.
4. **Chen L, Einbinder E, Zhang Q, Hasday J, Balke CW, Scharf SM.** Oxidative stress and left ventricular function with chronic intermittent hypoxia in rats. *Am J Respir Crit Care Med* 172: 915–920, 2005.
5. **Chen L, Zhang J, Gan TX, Chen-Izu Y, Hasday JD, Karmazyn M, Balke CW, Scharf SM.** Left ventricular dysfunction and associated cellular injury in rats exposed to chronic intermittent hypoxia. *J Appl Physiol* 104: 218–223, 2008.
6. **Christl SU, Murgatroyd PR, Gibson GR, Cummings JH.** Production, metabolism, and excretion of hydrogen in the large intestine. *Gastroenterology* 102: 1269–1277, 1992.
7. **Cortez DM, Feldman MD, Mummidi S, Valente AJ, Steffensen B, Vincenti M, Barnes JL, Chandrasekar B.** IL-17 stimulates MMP-1 expression in primary human cardiac fibroblasts via p38 MAPK- and

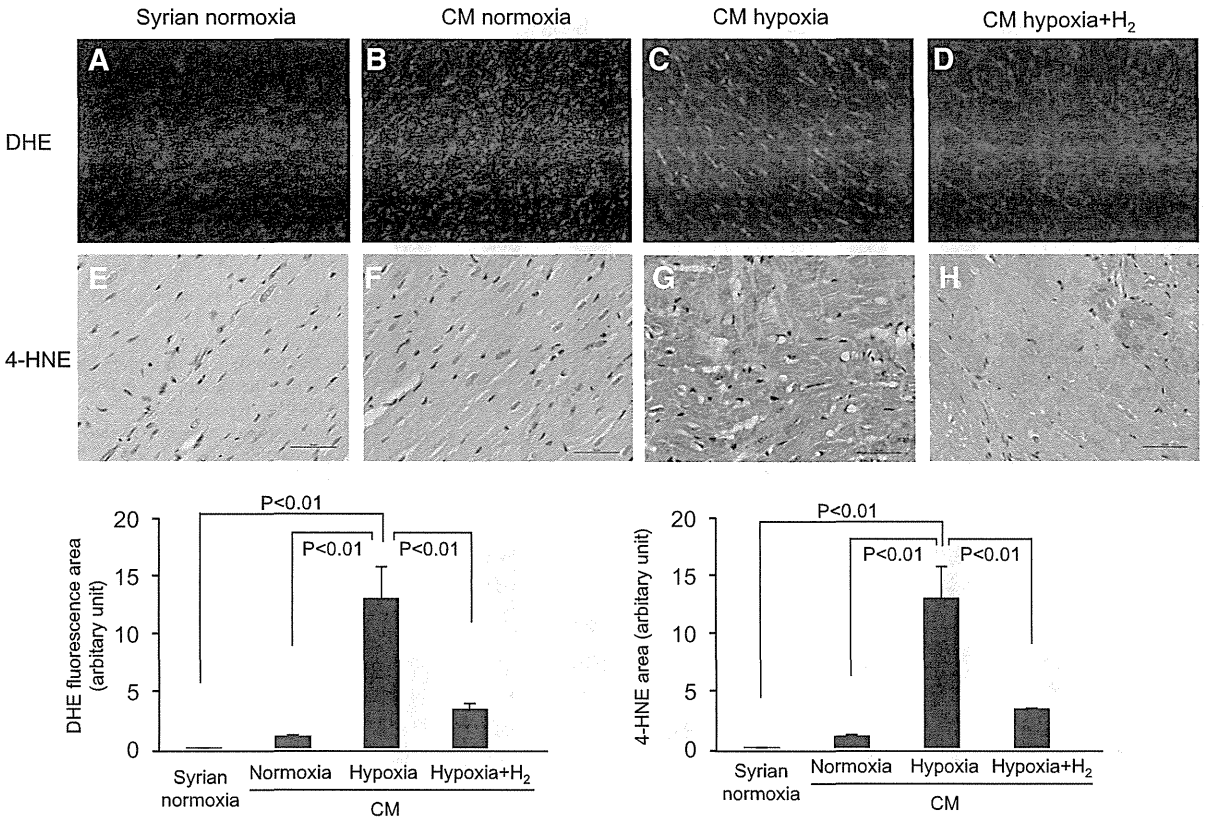

Fig. 5. Dihydroethidium (DHE) labeling (*A–D*) and immunohistochemistry for 4-hydroxy-2-nonenal (4-HNE; *E–G*) in LV myocardium of CM hamsters. Superoxide production (*C*) and oxidative stress (*G*) are increased in CM hamsters exposed to intermittent hypoxic stress, whereas these changes are suppressed by inhalation of hydrogen gas (*D* and *H*). Intermittent hypoxia significantly increased the levels of superoxide and 4-HNE-modified protein adducts in the LV myocardium, whereas inhaling hydrogen gas significantly reversed these changes. Values are shown as means ± SE (n = 4–7).

ERK1/2-dependent C/EBP-beta, NF-kappaB, and AP-1. *Am J Physiol Heart Circ Physiol* 293: H3356–H3365, 2007.

8. **Duran JM, Makarewich CA, Trappanese D, Gross P, Husain S, Dunn J, Lal H, Sharp TE, Starosta T, Vagnozzi RJ, Berretta RM, Barbe M, Yu D, Gao E, Kubo H, Force T, Houser SR.** Sorafenib cardiotoxicity increases mortality after myocardial infarction. *Circ Res* 114: 1700–1712, 2014.
9. **Fan H, Sun B, Gu Q, Lafond-Walker A, Cao S, Becker LC.** Oxygen radicals trigger activation of NF-kappaB and AP-1 and upregulation of ICAM-1 in reperfused canine heart. *Am J Physiol Heart Circ Physiol* 282: H1778–H1786, 2002.
10. **Gottlieb DJ, Yenokyan G, Newman AB, O'Connor GT, Punjabi NM, Quan SF, Redline S, Resnick HE, Tong EK, Diener-West M, Shahar E.** Prospective study of obstructive sleep apnea and incident coronary heart disease and heart failure: the sleep heart health study. *Circulation* 122: 352–360, 2010.
11. **Hastings PC, Vazir A, Meadows GE, Dayer M, Poole-Wilson PA, McIntyre HF, Morrell MJ, Cowie MR, Simonds AK.** Adaptive servo-ventilation in heart failure patients with sleep apnea: a real world study. *Int J Cardiol* 139: 17–24, 2010.
12. **Hayashi T, James TN, Buckingham DC.** Ultrastructure and immunohistochemistry of the coronary chemoreceptor in human and canine hearts. *Am Heart J* 129: 946–959, 1995.
13. **Hayashi T, Yoshioka T, Hasegawa K, Miyamura M, Mori T, Ukimura A, Matsumura Y, Ishizaka N.** Inhalation of hydrogen gas attenuates left ventricular remodeling induced by intermittent hypoxia in mice. *Am J Physiol Heart Circ Physiol* 301: H1062–H1069, 2011.
14. **Hsu TC, Young MR, Cmarik J, Colburn NH.** Activator protein 1 (AP-1)- and nuclear factor kappaB (NF-kappaB)-dependent transcriptional events in carcinogenesis. *Free Radic Biol Med* 28: 1338–1348, 2000.
15. **Inamoto S, Yoshioka T, Yamashita C, Miyamura M, Mori T, Ukimura A, Matsumoto C, Matsumura Y, Kitaura Y, Hayashi T.** Pitavastatin reduces oxidative stress and attenuates intermittent hypoxia-induced left ventricular remodeling in lean mice. *Hypertens Res* 33: 579–586, 2010.
16. **Ip MS, Tse HF, Lam B, Tsang KW, Lam WK.** Endothelial function in obstructive sleep apnea and response to treatment. *Am J Respir Crit Care Med* 169: 348–353, 2004.
17. **Javaheri S.** Heart failure. In: *Principles and Practice of Sleep Medicine* (5th ed.), edited by Kryger MH, Roth T, and Dement WC. St. Louis: Saunders, 2011, p. 1400–1415.
18. **Kasai T.** Sleep apnea and heart failure. *J Cardiol* 60: 78–85, 2012.
19. **Lattimore JD, Celermajer DS, Wilcox I.** Obstructive sleep apnea and cardiovascular disease. *J Am Coll Cardiol* 41: 1429–1437, 2003.
20. **Maeda H, Nagai H, Takemura G, Shintani-Ishida K, Komatsu M, Ogura S, Aki T, Shirai M, Kuwahira I, Yoshida K.** Intermittent-hypoxia induced autophagy attenuates contractile dysfunction and myocardial injury in rat heart. *Biochim Biophys Acta* 832: 1159–1166, 2013.
21. **Nadruz W, Jr., Kobarg CB, Kobarg J, Franchini KG.** c-Jun is regulated by combination of enhanced expression and phosphorylation in acute-overloaded rat heart. *Am J Physiol Heart Circ Physiol* 286: H760–H767, 2004.
22. **Nakao A, Sugimoto R, Billiar TR, McCurry.** Therapeutic antioxidant medical gas. *J Cli Biochem Nutr* 44: 1–13, 2009.
23. **Ohsawa I, Ishikawa M, Takahashi K, Watanabe M, Nishimaki K, Yamagata K, Katsura K, Katayama Y, Asoh S, Ohta S.** Hydrogen acts as a therapeutic antioxidant by selectively reducing cytotoxic oxygen radicals. *Nat Med* 13: 688–694, 2007.
24. **Ohta S.** Molecular hydrogen as a preventive and therapeutic medical gas: initiation, development and potential of hydrogen medicine. *Pharmacol Ther* 144: 1–11, 2014.
25. **Okuda N, Ito T, Emura N, Suwa M, Hayashi T, Yoneda H, Kitaura Y.** Depressed myocardial contractile reserve in patients with obstructive sleep

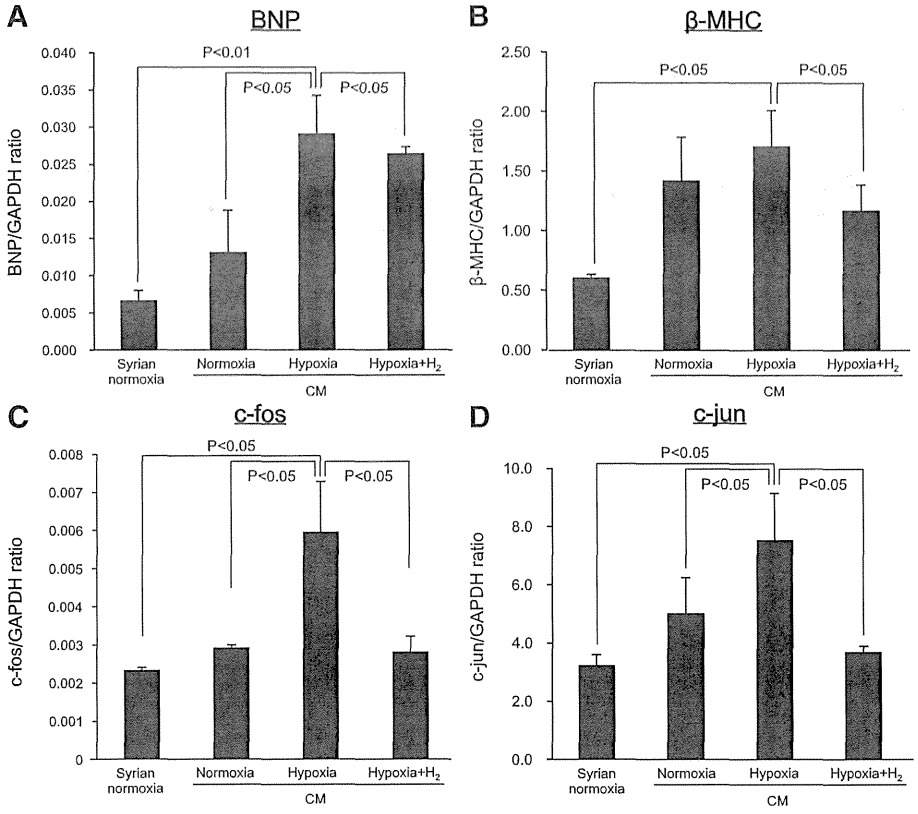

Fig. 6. Expression of mRNA for brain natriuretic peptide (BNP; *A*), β-myosin heavy chain (β-MHC; *B*), c-*fos* (*C*), and c-*jun* (*D*) in CM hamsters. Intermittent hypoxia significantly increased the expression of BNP, β-MHC, c-*fos*, and c-*jun* mRNA in the LV myocardium, whereas inhalation of hydrogen gas significantly reduced mRNA expression. GAPDH, glyceraldehyde-3-phosphate dehydrogenase. Values are shown as means ± SE (n = 4–9).

apnea assessed by tissue Doppler imaging with dobutamine stress echocardiography. *Chest* 131: 1082–1089, 2007.

26. **Partinen M, Guilleminault C.** Daytime sleepiness and vascular morbidity at seven-year follow-up in obstructive sleep apnea patients. *Chest* 97: 27–32, 1990.
27. **Roberts CK, Sindhu KK.** Oxidative stress and metabolic syndrome. *Life Sci* 54: 705–712, 2009.
28. **Sakamoto A, Abe M, Masaki T.** Delineation of genomic deletion in cardiomyopathic hamster. *FEBS Lett* 447: 124–128, 1994.
29. **Sakamoto A, Sugamoto Y.** Identification of a novel aldose reductase-like gene upregulated in the failing heart of cardiomyopathic hamster. *Mol Cell Biochem* 353: 275–281, 2011.
30. **Shen G, Jeong WS, Hu R, Kong AN.** Regulation of Nrf2, NF-kappaB, and AP-1 signaling pathways by chemopreventive agents. *Antioxid Redox Signal* 7: 1648–1663, 2005.
31. **Vatta M, Sinagra G, Brunelli L, Faulkner G.** Remodeling of dystrophin and sarcomeric Z-band occurs in pediatric cardiomyopathies: a unifying mechanism for force transmission defect. *J Cardiovasc Med* 10: 149–156, 2009.
32. **Williams AL, Chen L, Scharf SM.** Effects of allopurinol on cardiac function and oxidant stress in chronic intermittent hypoxia. *Sleep Breath* 14: 51–57, 2010.
33. **Yamashita C, Hayashi T, Mori T, Tazawa N, Kwak CJ, Nakano D, Sohmiya K, Okada Y, Kitaura Y, Matsumura Y.** Angiotensin-II receptor blocker reduces oxidative stress and attenuates hypoxia-induced left ventricular remodeling in apolipoprotein E-knockout mice. *Hypertens Res* 30: 1219–1230, 2007.
34. **Yoshiyama M, Takeuchi K, Hanatani A, Shimada T, Takemoto Y, Shimizu N, Omura T, Kim S, Iwao H, Yoshikawa J.** Effect of cilazapril on ventricular remodeling assessed by Doppler-echocardiographic assessment and cardiac gene expression. *Cardiovasc Drugs Ther* 12: 57–70, 1998.

Atherosclerosis 237 (2014) 301–306

Contents lists available at ScienceDirect

Atherosclerosis

journal homepage: www.elsevier.com/locate/atherosclerosis

Association between chronic kidney disease and thoracic aortic atherosclerosis detected using transesophageal echocardiography

Yoshiki Matsumura*, Kenichi Sugioka, Suwako Fujita, Asahiro Ito, Shinichi Iwata, Minoru Yoshiyama

Department of Cardiovascular Medicine, Osaka City University Graduate School of Medicine, 1-4-3, Asahi-machi, Abeno-ku, Osaka 545-8585, Japan

ARTICLE INFO

Article history:
Received 8 January 2014
Received in revised form
27 August 2014
Accepted 15 September 2014
Available online 30 September 2014

Keywords:
Aorta
Atherosclerosis
Kidney
Echocardiography

ABSTRACT

Objective: Accelerated atherosclerosis occurs with a high frequency in patients with chronic kidney disease (CKD). We evaluated the association between CKD and thoracic aortic plaques using transesophageal echocardiography (TEE). **Methods:** This study population consisted of 297 patients who underwent TEE. Aortic plaques were evaluated in the proximal thoracic aorta (PTA) (from the ascending aorta to the aortic arch) and the distal thoracic aorta (DTA) (the descending aorta) using TEE. Aortic plaques were defined as complex plaques of ≥4 mm thickness and with ulceration or mobile components. CKD was defined as the estimated glomerular filtration rate (eGFR) <60 mL/min/1.73 m^2. The association between CKD and aortic plaques was evaluated using multivariate analysis after adjusting for traditional atherosclerotic risk factors. **Results:** Patients with CKD ($n = 144$) had a higher incidence of any plaques and complex plaques compared with those without CKD ($n = 153$) (85% vs. 47% and 42% vs. 17%, respectively, both $P < 0.001$). Univariate analysis indicated that the presence of CKD was significantly associated with complex plaques both in the DTA and the PTA (both, $P < 0.001$); however, multivariate analysis indicated that the presence of CKD was associated with only complex plaques in the DTA ($P < 0.05$), but not with those in the PTA. **Conclusion:** The presence of CKD was associated with complex aortic plaques, with this association being stronger for complex plaques in the DTA than those in the PTA.

1. Introduction

Aortic atherosclerosis is a known marker of vascular disease and is associated with ischemic stroke, peripheral embolization, and coronary event [1–6]. The advent of multi-plane transesophageal echocardiography (TEE) has facilitated the diagnosis of aortic atherosclerosis, and it has become the standard technique for evaluating the degree of atherosclerosis severity [7,8]. The presence of aortic plaques, in particular complex plaques, which are detected using TEE, is associated with cardiovascular events and deaths [9–11]. Previous studies demonstrated that, in the general population, the number of any or complex aortic plaque increases distally from the ascending aorta [12–15]. The clinical implication of aortic plaques could be different depending on their location in the aorta. For example, compared to those in the descending aorta, complex plaques in the ascending aorta and aortic arch may be more closely associated to ischemic stroke (except in case with coincident severe aortic insufficiency). Additionally, studies in patients with coronary artery disease (CAD) found that the incidence of plaque was the lowest in the ascending aorta and increased in the aortic arch and the descending aorta [16,17]. Recently, chronic kidney disease (CKD), which has emerged as a major cardiovascular risk factor [18–21], has been associated with the presence of aortic atherosclerosis [22,23]. However, no prior study has evaluated the association between the degree of CKD and the severity of aortic atherosclerosis in every location in the thoracic aorta using TEE. The purpose of this study was to determine the association between the presence of CKD and the presence and location of atherosclerotic plaques in the thoracic aorta evaluated using TEE.

2. Methods

2.1. Study population

The study population consisted of 337 consecutive patients who were referred for clinically indicated TEE. We excluded 40 patients who met the following criteria: (1) 16 patients who had undergone previous cardiac or aortic surgery, (2) 15 who had endocarditis or

* Corresponding author.
E-mail address: matsumura@med.osaka-cu.ac.jp (Y. Matsumura).

http://dx.doi.org/10.1016/j.atherosclerosis.2014.09.013
0021-9150/

aortic artery disease such as thoracic aortic aneurysm or aortic dissection, (3) 5 who had unstable renal function or acute renal failure from any cause, and (4) 4 for whom TEE images were inadequate for evaluating aortic plaques and in whom the aortic arch could not be visualized fully by TEE. Finally, we included 297 patients (176 men, mean age: 66 ± 12 years) in this study. The hospital ethics committee approved the study protocol, and all patients gave their written informed consent prior to undergoing the TEE procedure.

The clinical data and history of atherosclerotic risk factors were obtained for each patient. Laboratory data were recorded from a time frame closest to that of the TEE. Hypertension was defined by a systolic blood pressure of >140 mmHg and/or a diastolic blood pressure of >90 mmHg or the use of antihypertensive medications. Diabetes mellitus was determined according to the presence of an existing diagnosis, a fasting blood glucose level of >6.99 mmol/L, IFCC-glycated hemoglobin A1c >47.5 mmol/mol, or the use of antidiabetic medications or insulin. Hypercholesterolemia was determined on the basis of a serum cholesterol level of >5.69 mmol/L or the use of cholesterol-lowering medications. Patients were classified as nonsmokers if they had never smoked or if they had stopped smoking for ≥1 year before the study, and all other patients were classified as smokers. CAD was defined as a history of previous myocardial infarction and/or percutaneous coronary intervention. Previous cerebral infarction and peripheral vascular disease were determined according to the data available from their medical records.

2.2. Transesophageal echocardiographic study

All patients underwent TEE using a multiplane transducer with a commercial ultrasound imaging system. The ascending and descending aorta and the aortic arch in the thoracic aorta were visualized in all patients. The aortic arch was defined as the portion of the aorta between the curve at the end of the ascending aorta and the origin of the left subclavian artery. The ascending aorta and aortic arch were classified as proximal thoracic aorta (PTA), and the descending aorta as distal thoracic aorta (DTA). Atherosclerotic plaques were defined as discrete protrusions of the intimal surface of the vessel of thickness of at least 2 mm, and these protrusions have a different appearance and echogenicity from the adjacent intact intimal surface [24–26]. The presence and location of any plaque were recorded. An ulceration was defined as a discrete indentation of the luminal surface of the plaque with a base width and maximum depth of ≥2 mm each [25,26]. Plaques were defined as complex if they were protruding and atheromatous with ≥4 mm thickness, mobile components, and plaque ulceration (Fig. 1) [12,26]. Plaques of <4 mm thickness and lacked morphologic features of complex atherosclerosis were considered as noncomplex plaques (Fig. 1). In the case of multiple plaques, the most advanced lesion was considered. The interpretation of echocardiographic studies was performed by an experienced echocardiographer who was blinded to the patient information.

2.3. Evaluation of renal function

The estimated glomerular filtration rate (eGFR) was calculated as $0.741 \times 175 \times \text{age}^{-0.203} \times (\text{serum creatinine})^{-1.154} \times (0.742$ if female) mL/min/1.73 m^2 [27]. CKD was defined as eGFR <60 mL/min/1.73 m^2. The degree of renal dysfunction was graded as follows: CKD stage 1, minimal damage to kidneys with normal renal function, eGFR ≥90 mL/min/1.73 m^2; CKD stage 2, mild renal dysfunction, 60 ≤ eGFR <90 mL/min/1.73 m^2; CKD stage 3, moderate renal dysfunction, 30 ≤ eGFR <60 mL/min/1.73 m^2; CKD stage 4, severe renal dysfunction, 15 ≤ eGFR <30 mL/min/1.73 m^2; CKD stage 5, end-stage renal dysfunction, eGFR <15 mL/min/1.73 m^2 or dialysis [28].

2.4. Statistical analysis

Clinical characteristics were expressed as mean ± standard deviation or number (percentage). Student unpaired *t* test or Mann–Whitney *U* test was used for comparison of mean values between 2 groups, as appropriate. All categorical values were compared using either the chi-square or Fisher exact test. The incidence of aortic plaque in all segments of the thoracic aorta was compared with the severity of renal dysfunction using the chi-square test and residual analysis. The associations between eGFR and the maximum thickness of plaque in each PTA and DTA were evaluated by the linear regression analysis. Univariate logistic regression analysis was used to assess the association of clinical factors and the presence of any or complex aortic plaques. Multivariate stepwise regression analysis was then used to assess the association between the presence of aortic plaques and the atherosclerotic factors, such as age, gender (men), body mass index, hypertension, diabetes mellitus, hypercholesterolemia, smoking, CAD, previous cerebral infarction, and CKD. Significant variables for univariate analysis were entered into the models. Age and body mass index were entered as a continuous variable in regression analysis. The values of $P < 0.05$ were considered statistically

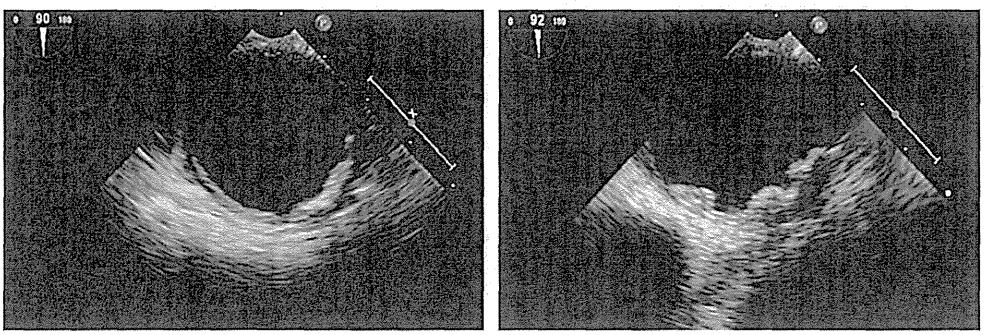

Fig. 1. Example images of noncomplex and complex aortic plaques detected using transesophageal echocardiography. PTA indicates proximal thoracic aorta.

significant. Statistical analysis was performed with SPSS 11.0 for Windows (SPSS Inc., Chicago, IL).

3. Results

The clinical indications for TEE were: the detection of a cardiac source of embolism or screening procedure before intervention in the electrophysiologic laboratory in 81 patients, evaluation of valvular heart disease in 185 patients (102 had aortic valve disease and 83 had mitral valve disease), congenital heart disease in 19 patients, intracardiac mass in 5 patients, and other reasons in 7 patients. Thirty-seven patients of 297 had CKD stage 1, 116 had CKD stage 2, 107 had CKD stage 3, 13 had CKD stage 4, and 24 had CKD stage 5. A total of 144 patients with CKD stages 3–5 were classified into the CKD group. The patients' clinical characteristics are listed in Table 1.

Patients with CKD were older, had a significantly higher prevalence of hypertension, diabetes mellitus, coronary artery disease, previous cerebral infarction, and peripheral vascular disease (all, $P < 0.05$) (Table 1). Patients with CKD had a significantly higher incidence of any aortic (85% vs. 47%, $P < 0.001$), noncomplex (44% vs. 30%, $P < 0.05$), and complex plaques (42% vs. 17%, $P < 0.001$) compared to those without CKD. Any plaque and noncomplex and complex plaques were observed with significantly greater frequency in both the PTA and the DTA in patients with CKD (Fig. 2). The incidence of any, noncomplex, and complex plaques in all the segments of the thoracic aorta in each groups categorized according to the severity of renal dysfunction is shown in Fig. 3. There was a significant association between the incidence of any and complex plaques and the severity of renal dysfunction (Fig. 3). Furthermore, there was significant association between the maximum plaque thickness and eGFR in both of the PTA ($r = -0.36$, $P < 0.001$) and DTA ($r = -0.48$, $P < 0.001$).

Univariate analysis indicated that complex plaques were associated with age, hypertension, diabetes mellitus, smoking, history of CAD, and CKD in all segments of thoracic aorta (Table 2). Multivariate analysis indicated that age, smoking, history of CAD, and CKD were independently associated with complex plaques in all segments (Table 2). In the analysis of each segment, univariate analysis indicated that complex plaques were associated with age, male gender, hypertension, diabetes mellitus, history of CAD, and CKD in the DTA (Table 3), and with age, hypertension, smoking, CAD, and CKD were in the PTA (Table 3). Multivariate analysis indicated that CKD was independently associated with complex plaques in the DTA ($P = 0.01$), but not with those in the PTA (Table 3).

For the evaluation of age and gender matched group data, we have selected 77 patients with CKD and 77 without CKD from our large cohort of patients (both groups, 39 men, mean age: 68 ± 9 years). In comparison between these matched groups, patients with CKD had a significantly higher prevalence of coronary artery disease (29% vs. 12%, $P < 0.01$) and peripheral vascular disease (8% vs. 0%, $P < 0.05$). Patients with CKD had a significantly higher incidence of any aortic (86% vs. 61%, $P < 0.001$), and complex plaques (42% vs. 23%, $P < 0.05$) in all segments of thoracic aorta, but not noncomplex plaques (44% vs. 38%, $P = 0.4$). Any and complex plaques were observed with significantly greater frequency in both the PTA (any plaques: 58% vs. 39%, $P < 0.05$; complex plaques: 29% vs. 14%, $P < 0.05$) and the DTA (any plaques: 78% vs. 49%, $P < 0.001$; complex plaques: 40% vs. 17%, $P < 0.005$) in patients with CKD.

Table 1
Clinical characteristics.

Variable	No CKD ($n = 153$)	CKD ($n = 144$)	P
Age (years)	61 ± 14	71 ± 8	<0.001
Male gender	93 (61%)	83 (58%)	0.58
Body mass index	22 ± 4	22 ± 3	0.82
Hypertension	77 (50%)	99 (69%)	0.002
Diabetes mellitus	30 (20%)	51 (35%)	0.002
Hypercholesterolemia	48 (31%)	58 (40%)	0.13
Smoking	38 (25%)	42 (29%)	0.44
Coronary artery disease	13 (9%)	40 (28%)	<0.001
Previous cerebral infarction	11 (7%)	23 (16%)	0.02
Peripheral vascular disease	0 (0%)	11 (8%)	0.001
eGFR (mL/min/1.73 m^2)	80 ± 15	39 ± 18	<0.001

CKD, chronic kidney disease; eGFR, estimated glomerular filtration rate.

4. Discussion

This present study shows that patients with CKD had a significantly higher incidence of any and complex aortic plaques compared to those without CKD. There was a strong association between the severity of atherosclerosis in the thoracic aorta and the degree of renal dysfunction. Furthermore, multivariate analysis indicated that age and history of CAD were independently associated with the presence of complex plaques in both the DTA and the PTA. However, the presence of CKD was independently associated with the presence of complex plaques in the DTA, but not that in the PTA. To the best of our knowledge, this is the first study to show an association between the aortic complex plaques evaluated using TEE and the severity of CKD in each location of the thoracic aorta.

Our study demonstrated that the severity of aortic atherosclerosis is strongly associated with the severity of renal dysfunction. These findings are consistent with those obtained in the studies by Haruki et al. [22] and Desai et al. [23] In both the reports, the severity of atherosclerosis in the thoracic aorta (predominantly the descending aorta) was closely associated with the degree of renal dysfunction. However, neither study showed the incidence of complex plaques in each location of thoracic aorta. Haruki et al. evaluated the severity of aortic atherosclerosis only in the descending aorta, and not in the ascending aorta or aortic arch. Although Desai et al. described that aortic atherosclerosis, in particular in the DTA, was associated with the severity of renal dysfunction, they did not study the difference in the association of renal dysfunction between aortic atherosclerosis in the DTA and that in the PTA. In this study, we demonstrated the association between aortic atherosclerosis and renal dysfunction in each location of the thoracic aorta. Complex plaques are association with the presence of CKD and are independent of any other atherosclerotic risk factors in the DTA, while not in the PTA.

We found that incidence of any and complex plaques was lower in the PTA and higher in the DTA in patients with CKD. Furthermore, complex plaques only in the DTA were independently associated with the presence of CKD. Several mechanisms can be speculated based on our findings. The first mechanism may be the embolization of thrombus or atherosclerosis from the aortic complex plaques to the renal vasculature. Previous studies have reported that aortic atherosclerotic lesions are recognized as an essential cause of systemic embolization, including ischemic stroke or peripheral embolization [29–32]. Although the cause of renal dysfunction is known to be multifactorial, the embolization from the aortic complex plaques in the DTA could be one of the causes of renal impairment. Aortic atherosclerosis in the PTA may also cause the showering of atheroemboli in the renal vasculature [32]. However, because complex plaques which cause peripheral embolization in the DTA are more frequent and anatomically closer to the renal artery than those in the PTA, it is possible that aortic atherosclerosis in the DTA is closely related to renal dysfunction rather than that in the PTA.

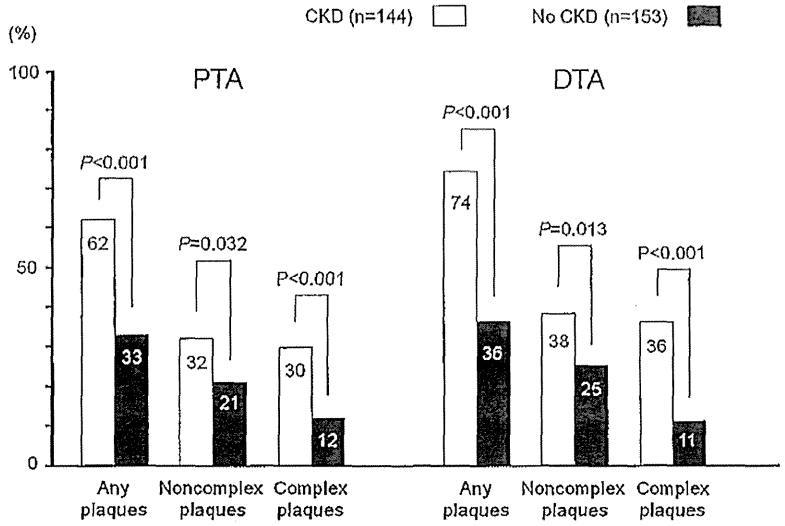

Fig. 2. Prevalence of aortic plaques in the PTA and the DTA in patients with and without CKD. "Noncomplex plaques" means only noncomplex plaques without complex plaque. "Complex plaques" means at least one or more complex plaque. Any plaque and noncomplex and complex plaques were seen with significantly greater frequency in both of the PTA and the DTA in patients with CKD. DTA indicates distal thoracic aorta; PTA, proximal thoracic aorta; and CKD, chronic kidney disease.

The other mechanism may be the association between CKD and systemic atherosclerosis. After considering atherosclerosis as a systemic disease, the calculation of the degree of severity of aortic plaques should reflect the total burden of atherosclerotic disease. Previous investigators demonstrated that in the general population, the number of any or complex aortic plaques increased distally from the ascending aorta [12–14]. Kronzon et al. [12] reported that complex aortic plaques were observed in the ascending aorta in only 0.2% patients and in the aortic arch in only 2.2%, and most of the complex plaques were found in the descending aorta, that is, in 6.0% of a relatively elderly and homogeneous (white) population.

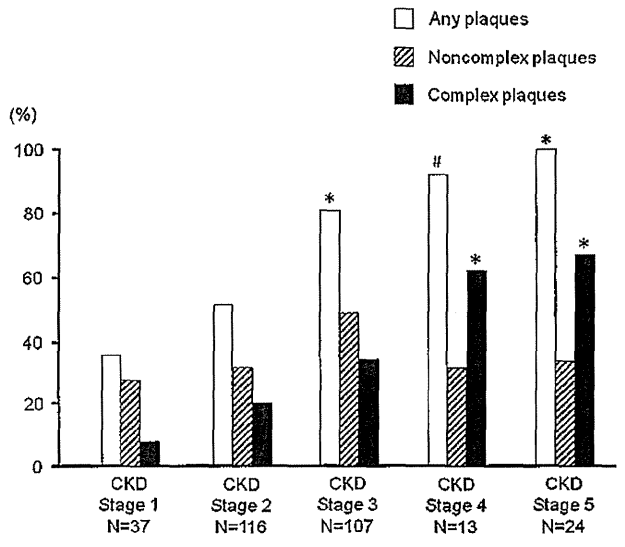

Fig. 3. Incidence of aortic plaques in each groups categorized according to the severity of renal dysfunction. See previous figure for an explanation of noncomplex and complex plaques. There were significant differences of the incidence of any and complex plaques between the each groups categorized by CKD stages (both, $P < 0.001$), but those of noncomplex plaques were not ($P = 0.063$). $^{*}P < 0.01$ versus CKD stage 1 group. $^{\#}P < 0.05$ versus CKD stage 1 group.

Although the differences in aortic arch geometry, hemodynamics, and wall shear stress may influence the incidence of complex aortic plaques, the true cause is not clear. However, the atherosclerotic process may begin earlier in the descending aorta than in the aortic arch or in the ascending aorta. Furthermore, the incidence of the complex plaques was lower in the PTA and higher in the DTA even in CAD patients with severe systemic atherosclerosis [17]. Therefore, complex aortic plaques in the DTA may reflect accelerated systemic atherosclerosis compared with those in the PTA. Although the complex plaques in the PTA were more important for risk stratification of stroke, those in the DTA were closely related marker for systemic atherosclerotic change. On the other hand, CKD has emerged as a major cardiovascular risk factor. Multiple possible explanations exist for the association between CKD and increased cardiovascular events. We observed an increased prevalence of prior cardiovascular disease, known risk factors for cardiovascular events, and coexisting conditions with CKD. However, CKD was independent and a strong risk factor for adverse outcomes. The association between CKD and increasing cardiovascular risk may be explained by multiple factors, including anemia, oxidative stress, abnormal calcium-phosphate homeostasis, enhanced coagulability, and inflammatory factors [33,34], all of which are associated with accelerated systemic atherosclerosis and endothelial dysfunction. Indeed, we found that incidence of complex plaque was lower in the PTA and higher in the DTA in patients with CKD, and that the association of CKD with severe atherosclerotic changes in the DTA was stronger than with the changes in the PTA.

4.1. Study limitations

Some limitations of this study should be addressed. Although this study population consisted of a consecutive series of patients who were referred for clinically indicated TEE, a potential selection bias may confound our results. The existence of a sonographic blind spot in the aorta (upper ascending aorta) is an additional limitation in this analysis which seeks to define plaque prevalence. The data of albuminuria or risk factors for CKD may help to evaluate the early phase of renal dysfunction (CKD stage 0). However, their data were not available because this study was a retrospective analysis. Long-

Table 2
Univariate and multivariate regression analysis for presence of complex plaques in all segments of thoracic aorta.

Variable	Univariate		Multivariate	
	OR (95% CI)	*P* value	OR (95% CI)	*P* value
Age (per year)	1.110 (1.074–1.147)	<0.001	1.076 (1.036–1.116)	<0.001
Male gender	1.609 (0.960–2.697)	0.07		
Body mass index	1.027 (0.960–1.099)	0.4		
Hypertension	3.063 (1.733–5.412)	<0.001	1.695 (0.871–3.299)	0.1
Diabetes mellitus	1.784 (1.039–3.063)	0.036	0.903 (0.469–1.739)	0.9
Hypercholesterolemia	1.281 (0.767–2.139)	0.3		
Smoking	1.972 (1.133–3.433)	0.016	2.009 (1.057–3.820)	0.03
Coronary artery disease	4.778 (2.561–8.914)	<0.001	2.590 (1.273–5.269)	0.009
Previous cerebral infarction	2.437 (0.620–9.581)	0.2		
Peripheral vascular disease	1.938 (0.576–6.521)	0.3		
Chronic kidney disease	3.733 (2.197–6.341)	<0.001	2.130 (1.118–4.059)	0.02

CI, confidence interval; OR, odds ratio.
See previous tables for an explanation of other abbreviations.

Table 3
Univariate and multivariate regression analysis for presence of complex plaques in the distal and proximal thoracic aorta.

Variable	Distal thoracic aorta				Proximal thoracic aorta			
	Univariate		Multivariate		Univariate		Multivariate	
	OR (95% CI)	*P* value	OR (95% CI)	*P* value	OR (95% CI)	*P* value	OR (95% CI)	*P* value
Age (per year)	1.088 (1.052–1.124)	<0.001	1.080 (1.037–1.124)	<0.001	1.118 (1.076–1.163)	<0.001	1.081 (1.035–1.129)	<0.001
Male gender	1.786 (1.004–3.175)	0.048	2.383 (1.209–4.696)	0.01	1.173 (0.658–2.093)	0.6		
Body mass index	1.039 (0.966–1.118)	0.3			1.007 (0.932–1.088)	0.9		
Hypertension	2.873 (1.528–5.399)	0.001	1.598 (0.782–3.269)	0.2	2.553 (1.330–4.901)	0.005	1.318 (0.621–2.798)	0.5
Diabetes mellitus	2.049 (1.153–3.639)	0.014	1.225 (0.639–2.347)	0.5	1.429 (0.774–2.639)	0.3		
Hypercholesterolemia	1.301 (0.746–2.269)	0.4			1.323 (0.741–2.362)	0.3		
Smoking	1.562 (0.859–2.843)	0.1			2.022 (1.081–3.785)	0.03	1.910 (0.950–3.837)	0.07
Coronary artery disease	4.994 (2.652–9.403)	<0.001	2.636 (1.307–5.317)	0.007	4.155 (2.182–7.912)	<0.001	2.506 (1.197–5.248)	0.02
Previous cerebral infarction	2.455 (0.618–9.759)	0.2			3.508 (0.885–13.905)	0.07		
Peripheral vascular disease	1.250 (0.322–4.846)	0.7			2.296 (0.650–8.112)	0.2		
Chronic kidney disease	4.522 (2.461–8.307)	<0.001	2.370 (1.207–4.655)	0.01	3.193 (1.739–5.863)	<0.001	1.792 (0.857–3.749)	0.1

See previous tables for an explanation of other abbreviations.

term follow-up studies were needed to evaluate the predictive value of complex plaques or renal dysfunction and determine the effect of medical treatment on plaque morphology or renal function.

5. Conclusion

Patients with CKD had a significantly higher incidence of any aortic and complex plaques compared with those without CKD. CKD was strongly associated with complex plaques in the DTA compared to that in the PTA. The association of complex aortic plaques with CKD may be different between the DTA and the PTA.

Disclosures

The authors have no funding, financial relationships, or conflicts of interest to disclose.

References

[1] Tunick PA, Kronzon I. Protruding atherosclerotic plaque in the aortic arch of patients with systemic embolization: a new finding seen by transesophageal echocardiography. Am. Heart J. 1990;120:658–60.
[2] Stone DA, Hawke MW, LaMonte M, Kittner SJ, Acosta J, Corretti M, Sample C, Price TR, Plotnick GD. Ulcerated atherosclerotic plaques in the thoracic aorta are associated with cryptogenic stroke: a multiplane transesophageal echocardiographic study. Am. Heart J. 1995;130:105–8.
[3] Atherosclerotic disease of the aortic arch as a risk factor for recurrent ischemic stroke. The French Study of Aortic Plaques in Stroke Group. N. Engl. J. Med. 1996;334:1216–21.
[4] Amarenco P, Cohen A, Tzourio C, Bertrand B, Hommel M, Besson G, Chauvel C, Touboul PJ, Bousser MG. Atherosclerotic disease of the aortic arch and the risk of ischemic stroke. N. Engl. J. Med. 1994;331:1474–9.
[5] Tunick PA, Rosenzweig BP, Katz ES, Freedberg RS, Perez JL, Kronzon I. High risk for vascular events in patients with protruding aortic atheromas: a prospective study. J. Am. Coll. Cardiol. 1994;23:1085–90.
[6] Tunick PA, Perez JL, Kronzon I. Protruding atheromas in the thoracic aorta and systemic embolization. Ann. Intern. Med. 1991;115:423–7.
[7] Daniel WG, Erbel R, Kasper W, Visser CA, Engberding R, Sutherland GR, Grube E, Hanrath P, Maisch B, Dennig K. Safety of transesophageal echocardiography. A multicenter survey of 10,419 examinations. Circulation 1991;83:817–21.
[8] McNamara RL, Lima JA, Whelton PK, Powe NR. Echocardiographic identification of cardiovascular sources of emboli to guide clinical management of stroke: a cost-effectiveness analysis. Ann. Intern. Med. 1997;127:775–87.
[9] Montgomery DH, Ververis JJ, McGorisk G, Frohwein S, Martin RP, Taylor WR. Natural history of severe atheromatous disease of the thoracic aorta: a transesophageal echocardiographic study. J. Am. Coll. Cardiol. 1996;27:95–101.
[10] Ferrari E, Vidal R, Chevallier T, Baudouy M. Atherosclerosis of the thoracic aorta and aortic debris as a marker of poor prognosis: benefit of oral anticoagulants. J. Am. Coll. Cardiol. 1999;33:1317–22.
[11] Izumi C, Takahashi S, Miyake M, Sakamoto J, Hanazawa K, Yoshitani K, Kaitani K, Izumi T, Gen H, Nakagawa Y. Impact of aortic plaque morphology on survival rate and incidence of a subsequent embolic event – long-term follow-up data. Circ. J. 2010;74:2152–7.
[12] Kronzon I, Tunick PA. Aortic atherosclerotic disease and stroke. Circulation 2006;114:63–75.
[13] Blackshear JL, Pearce LA, Hart RG, Zabalgoitia M, Labovitz A, Asinger RW, Halperin JL. Aortic plaque in atrial fibrillation: prevalence, predictors, and thromboembolic implications. Stroke 1999;30:834–40.
[14] Transesophageal echocardiographic correlates of thromboembolism in high-risk patients with nonvalvular atrial fibrillation. The Stroke Prevention in Atrial Fibrillation Investigators Committee on Echocardiography. Ann. Intern. Med. 1998;128:639–47.
[15] Strong JP, Malcom GT, McMahan CA, Tracy RE, Newman 3rd WP, Herderick EE, Cornhill JF. Prevalence and extent of atherosclerosis in adolescents and young

adults: implications for prevention from the Pathobiological Determinants of Atherosclerosis in Youth Study. JAMA 1999;281:727–35.
[16] Khoury Z, Gottlieb S, Stern S, Keren A. Frequency and distribution of atherosclerotic plaques in the thoracic aorta as determined by transesophageal echocardiography in patients with coronary artery disease. Am. J. Cardiol. 1997;79:23–7.
[17] Gu X, He Y, Li Z, Kontos MC, Paulsen WH, Arrowood JA, Vetrovec GW, Nixon JV. Relation between the incidence, location, and extent of thoracic aortic atherosclerosis detected by transesophageal echocardiography and the extent of coronary artery disease by angiography. Am. J. Cardiol. 2011;107:175–8.
[18] Shlipak MG, Fried LF, Cushman M, Manolio TA, Peterson D, Stehman-Breen C, Bleyer A, Newman A, Siscovick D, Psaty B. Cardiovascular mortality risk in chronic kidney disease: comparison of traditional and novel risk factors. JAMA 2005;293:1737–45.
[19] Go AS, Chertow GM, Fan D, McCulloch CE, Hsu CY. Chronic kidney disease and the risks of death, cardiovascular events, and hospitalization. N. Engl. J. Med. 2004;351:1296–305.
[20] Weiner DE, Tighiouart H, Stark PC, Amin MG, MacLeod B, Griffith JL, Salem DN, Levey AS, Sarnak MJ. Kidney disease as a risk factor for recurrent cardiovascular disease and mortality. Am. J. Kidney Dis. 2004;44:198–206.
[21] Sarnak MJ, Levey AS, Schoolwerth AC, Coresh J, Culleton B, Hamm LL, McCullough PA, Kasiske BL, Kelepouris E, Klag MJ, Parfrey P, Pfeffer M, Raij L, Spinosa DJ, Wilson PW, American Heart Association Councils on Kidney in Cardiovascular Disease, High Blood Pressure Research, Clinical Cardiology, and Epidemiology and Prevention. Kidney disease as a risk factor for development of cardiovascular disease: a statement from the American Heart Association Councils on Kidney in Cardiovascular Disease, High Blood Pressure Research, Clinical Cardiology, and Epidemiology and Prevention. Hypertension 2003;42:1050–65.
[22] Haruki N, Takeuchi M, Kaku K, Yoshitani H, Tamura M, Abe H, Okazaki M, Ota T, Otsuji Y. Prevalence and clinical implication of complex atherosclerotic plaque in the descending thoracic aorta of Japanese patients assessed by transesophageal echocardiography. Circ. J. 2010;74:2627–32.
[23] Desai MY, Kwon DH, Nair D, Mankad SV, Popovic Z, DeCastro S, Nasser HJ, Patel A, Kuvin J, Pandian NG. Association of aortic atherosclerosis and renal dysfunction. J. Am. Soc. Echocardiogr. 2008;21:751–5.
[24] Sugioka K, Hozumi T, Sciacca RR, Miyake Y, Titova I, Gaspard G, Sacco RL, Homma S, Di Tullio MR. Impact of aortic stiffness on ischemic stroke in elderly patients. Stroke 2002;33:2077–81.
[25] Di Tullio MR, Russo C, Jin Z, Sacco RL, Mohr JP, Homma S, Patent Foramen Ovale in Cryptogenic Stroke Study Investigators. Aortic arch plaques and risk of recurrent stroke and death. Circulation 2009;119:2376–82.
[26] Sugioka K, Matsumura Y, Hozumi T, Fujita S, Ito A, Kataoka T, Takagi M, Mizutani K, Naruko T, Hosono M, Hirai H, Sasaki Y, Ueda M, Suehiro S, Yoshiyama M. Relation of aortic arch complex plaques to risk of cerebral infarction in patients with aortic stenosis. Am. J. Cardiol. 2011;108:1002–7.
[27] Imai E, Horio M, Nitta K, Yamagata K, Iseki K, Tsukamoto Y, Ito S, Makino H, Hishida A, Matsuo S. Modification of the Modification of Diet in Renal Disease (MDRD) Study equation for Japan. Am. J. Kidney Dis. 2007;50:927–37.
[28] National Kidney Foundation. K/DOQI clinical practice guidelines for chronic kidney disease: evaluation, classification, and stratification. Am. J. Kidney Dis. 2002;39:S1–266.
[29] Kassirer JP. Atheroembolic renal disease. N. Engl. J. Med. 1969;280:812–8.
[30] Fine MJ, Kapoor W, Falanga V. Cholesterol crystal embolization: a review of 221 cases in the English literature. Angiology 1987;38:769–84.
[31] Coy KM, Maurer G, Goodman D, Siegel RJ. Transesophageal echocardiographic detection of aortic atheromatosis may provide clues to occult renal dysfunction in the elderly. Am. Heart J. 1992;123:1684–6.
[32] Dávila-Román VG, Kouchoukos NT, Schechtman KB, Barzilai B. Atherosclerosis of the ascending aorta is a predictor of renal dysfunction after cardiac operations. J. Thorac. Cardiovasc. Surg. 1999;117:111–6.
[33] Muntner P, Hamm LL, Kusek JW, Chen J, Whelton PK, He J. The prevalence of nontraditional risk factors for coronary heart disease in patients with chronic kidney disease. Ann. Intern. Med. 2004;140:9–17.
[34] Shlipak MG, Fried LF, Crump C, Bleyer AJ, Manolio TA, Tracy RP, Furberg CD, Psaty BM. Elevations of inflammatory and procoagulant biomarkers in elderly persons with renal insufficiency. Circulation 2003;107:87–92.

Heart Vessels
DOI 10.1007/s00380-014-0575-7

ORIGINAL ARTICLE

Long-term prognostic impact of the attenuated plaque in patients with acute coronary syndrome

Hiroyuki Okura · Toru Kataoka · Minoru Yoshiyama · Junichi Yoshikawa · Kiyoshi Yoshida

Received: 4 June 2014 / Accepted: 22 August 2014

Abstract Several intravascular ultrasound studies have reported that culprit lesion-attenuated plaque (AP) is related to slow flow/no reflow after percutaneous coronary intervention (PCI). Long-term prognostic impact of the AP is unknown. The aim of this study was to investigate acute and long-term clinical impact of the AP in patients with acute coronary syndrome (ACS). A total of 110 ACS patients who underwent successful PCI were enrolled. Acute and long-term clinical outcomes were compared between patients with AP (AP group: $n = 73$) and those without AP (non-AP group: $n = 37$). Long-term cardiac event was defined as a composite of death and ACS. Baseline characteristics in 2 groups were similar. AP was associated with higher TIMI frame count immediately after the first balloon inflation. After thrombectomy and intracoronary drug administration, final TIMI frame count became similar between AP and non-AP group. Although AP was associated with higher incidence of fatal arrhythmia during hospitalization, in-hospital mortality did not differ between the 2 groups. During follow-up (median 6.2 years), cardiac event-free survival did not differ between the 2 groups. Despite the initial unfavorable effect on coronary reflow, presence of AP did not affect acute as well as long-term clinical outcome in patients with ACS.

Keywords IVUS · Acute coronary syndrome · Atherosclerosis · Stent

H. Okura · T. Kataoka
The Division of Cardiology, Bell Land General Hospital, Sakai, Japan

H. Okura (✉) · K. Yoshida
The Division of Cardiology, Kawasaki Medical School, 577 Matsushima, Kurashiki 701-0192, Japan
e-mail: hokura@fides.dti.ne.jp

M. Yoshiyama
The Division of Internal Medicine and Cardiology, Osaka City University Graduate School of Medicine, Osaka, Japan

J. Yoshikawa
The Division of Internal Medicine and Cardiology, Nishinomiya Watanabe Cardiovascular Center, Nishinomiya, Japan

Introduction

Coronary arterial plaque with ultrasonic attenuation ("attenuated plaque") detected by intravascular ultrasound (IVUS) has been recognized as a high-risk plaque for slow flow/no reflow during percutaneous coronary intervention (PCI) [1–5]. IVUS-derived tissue characterization as well as pathological examinations have shown that attenuated plaque contains necrotic core and lipid components rather than fibrous tissue [3, 6, 7].

Although lesions with attenuated plaque have high risk for transient coronary flow deterioration and in-hospital complications following PCI in patients with acute coronary syndrome (ACS) [1], long-term prognostic impact of the attenuated plaque has not been fully investigated [8].

The aim of the current study was to investigate long-term prognostic impact of the attenuated plaque in patients with ACS.

Patients and methods

Study patients

Between January 2001 and December 2002, 110 acute coronary syndrome (ACS) patients (89 acute myocardial

Published online: 03 September 2014

infarction and 21 unstable angina pectoris) with intravascular ultrasound (IVUS) imaging were originally enrolled [1]. The diagnosis of ACS includes unstable angina pectoris, ST elevation myocardial infarction and non-ST elevation myocardial infarction. There were 82 male and 28 female, mean age of 63 ± 9 years. Long-term clinical outcome of the originally investigated patients was retrospectively reviewed and investigated. Written informed consent was obtained from all patients at the time of the initial enrollment. Study protocol was approved by the internal review board.

Angiographic and IVUS procedure

Angiographic and IVUS procedures were reported previously [1]. In brief, coronary angiography was performed by the femoral or radial approach. After diagnostic angiography, IVUS pullback imaging was performed and repeated after PCI using an automated pullback device (0.5 mm/s). After PCI, patients were maintained on a regimen of aspirin (81–100 mg daily) plus ticlopidine (200 mg daily) for 4 weeks or longer.

Angiographic analyses

Angiographic coronary flow was assessed at (1) baseline, (2) immediately after the first balloon inflation, and (3) after all PCI procedures, using TIMI flow grade and TIMI frame count. Quantitative coronary angiography was performed using a commercially available system, CMS-QCA (MEDIS, Leiden, Netherlands).

IVUS analyses

The IVUS images were recorded on SVHS videotape. Quantitative IVUS measurements were performed at the culprit lesion segment as well as at proximal and distal reference segments, which were defined as most normal looking sites within 10 mm from the culprit lesion. External elastic membrane cross-sectional area (EEM CSA) and lumen cross-sectional area (Lumen CSA) were measured using commercially available planimetry software (NetraIVUS, SC Image Inc., Los. Alto, CA). Plaque plus media cross-sectional area (P + M CSA) was calculated as the difference between EEM and lumen CSA. Plaque burden was calculated as P + M CSA/EEM CSA × 100 at the culprit segment. Plaque type was categorized into two types according to the presence (AP group) or absence (non-AP group) of ultrasonic attenuation (Fig. 1).

In-hospital clinical outcome

Patients were monitored during hospitalization (<30 days) for the occurrence of complications, such as recurrent

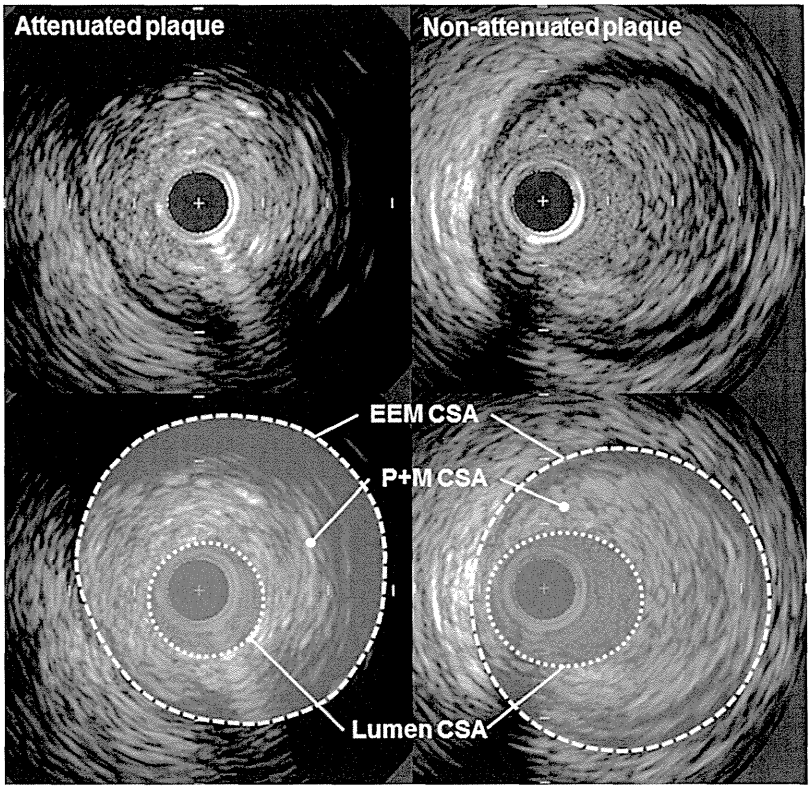

Fig. 1 Attenuated plaque and non-attenuated plaque. Example IVUS images of attenuated plaque (*left*) and non-attenuated plaque (*right*) with quantitative measurements. *EEM CSA* external elastic membrane cross-sectional area, *Lumen CSA* lumen cross-sectional area, *P + M CSA* plaque plus media cross-sectional area

Table 1 Medications at discharge

	Attenuated plaque ($n = 73$)	Non-attenuated plaque ($n = 37$)	P value
Aspirin [n (%)]	73 (100)	37 (100)	–
Ticlopidine [n (%)]	61 (84)	30 (81)	0.75
ACEI or ARB [n (%)]	48 (66)	13 (35)	<0.01
Beta-blockers [n (%)]	15 (21)	5 (14)	0.37
Ca channel blockers [n (%)]	9 (12)	4 (11)	0.82
Nitrates [n (%)]	34 (47)	12 (32)	0.16
Statin [n (%)]	19 (26)	8 (22)	0.61

ACEI angiotensin-converting enzyme inhibitors, *ARB* angiotensin receptor blockers

myocardial infarction, congestive heart failure, fatal arrhythmia (ventricular tachycardia, ventricular fibrillation, or complete atrioventricular block), cardiac rupture, stroke or cardiac death. Serum creatine phosphokinase (CPK) level was measured serially every 3 h after PCI until the peak value was achieved.

Clinical follow-up

Clinical events were confirmed by a chart review and/or telephone contact. Primary endpoint was major adverse cardiac events (MACE) defined as a composite of all-cause death and ACS. ACS was defined as ST elevation myocardial infarction, non-ST elevation myocardial infarction or unstable angina pectoris.

Statistical analysis

Quantitative data are presented as mean ± SD. Differences between groups were analyzed by Student's unpaired t test. Categorical variables were compared by Chi-square analysis. Statistical significance was defined as $P < 0.05$. All statistical analyses were performed with Statview version 5 (SAS Institutes).

Results

Clinical characteristics

Attenuated plaque was documented in 73 lesions from 73 patients. Baseline clinical characteristics, angiographic and IVUS results comparing AP group ($n = 73$) and non-AP group ($n = 37$) were previously reported [1]. In brief, clinical characteristics were similar between the 2 groups, except for a higher prevalence of hyperlipidemia in the AP group ($P = 0.05$). By IVUS, EEM CSA and P + M CSA were significantly greater in the AP group than in the non-AP group (EEM CSA: 18.8 ± 5.4 vs. 14.2 ± 4.8 mm^2, $P < 0.01$, P + M CSA: 16.6 ± 5.2 vs. 11.6 ± 4.5 mm^2, $P < 0.01$). On the other hand, lumen CSA before stenting (2.2 ± 0.4 vs. 2.2 ± 0.6 mm^2, $P = 0.86$) was similar between the 2 groups. By angiography, TIMI frame count was similar between the AP and non-AP groups at baseline (53.7 vs. 60.5, P = NS). Although TIMI frame count immediately after the first balloon dilatation was significantly higher in the AP group than in the non-AP group (45.7 vs. 35.3, $P = 0.03$), final TIMI frame count (32.1 vs. 33, P = NS) was similar between the 2 groups. TIMI 3 flow was achieved in 93 % of the AP group and in 100 % of the non-AP group ($P = 0.10$) [1].

Baseline medications at discharge are summarized in Table 1. Aspirin was used in all patients and dual antiplatelets were continued in >80 %. Angiotensin-converting enzyme inhibitors or angiotensin receptor blockers were more frequently used in patients with AP (66 vs. 35 %, $P < 0.01$). Otherwise, no significant differences in medications were documented.

In-hospital and long-term clinical follow-up

In-hospital events were also reported previously. Death (3 vs. 3 %, $P = 0.99$) and congestive heart failure (8 vs. 3 %, $P = 0.51$) were similarly observed in the 2 groups. Fatal arrhythmia was more frequently documented in the AP group than in the non-AP group (16 vs. 3 %, $P = 0.04$) [1].

Long-term clinical events are summarized in the Table 2. During follow-up (median 6.2 years), incidence of all-cause death, cardiac death, non-cardiac death, congestive heart failure, and acute coronary syndrome were similar between the 2 groups.

By Kaplan–Meier analysis, event-free survival rate was also similar between the 2 groups (Fig. 2).

Discussion

Despite its negative impact on coronary reflow, attenuated plaque was not associated with poor long-term clinical outcome. Our present results were, in part, concordant with a previous study [8]. Xu et al. [8] reported natural course and prognosis of the attenuated plaque in patients with acute myocardial infarction from the HORIZONS-AMI. At 3-year follow-up, attenuated plaque was not associated

Table 2 Long-term clinical events

	Attenuated plaque ($n = 73$)	Non-attenuated plaque ($n = 37$)	P value
Follow-up period (years)	7.1 ± 3.1	6.5 ± 3.6	0.36
All-cause death [n (%)]	8 (11)	2 (5)	0.34
Cardiac death [n (%)]	6 (8)	1 (3)	
Non-cardiac death [n (%)]	2 (3)	1 (3)	
ACS [n (%)]	9 (12)	6 (16)	0.57
STEMI [n (%)]	6 (8)	4 (11)	
Non-STEMI [n (%)]	0 (0)	0 (0)	
Unstable angina [n (%)]	3 (4)	2 (5)	
All-cause death ± ACS [n (%)]	15 (21)	7 (19)	0.84
Congestive heart failure [n (%)]	5 (7)	1 (3)	0.37

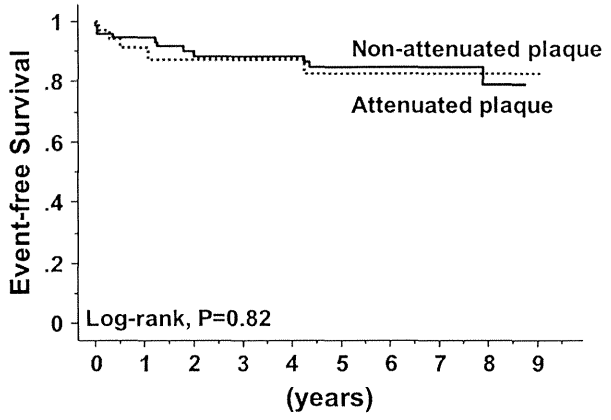

Fig. 2 Event-free survival curves. The Kaplan–Meier curves showed that cardiac event-free survival was similar between patients with attenuated plaque and non-attenuated plaque (Log-rank, $P = 0.82$)

with increased risk of major adverse clinical outcome. Although attenuated plaque was reported correlated with no-reflow during PCI in the previous report from the same study population [5], incidence of final TMI-3 flow was reported similar between patients with and without attenuated plaque [8]. Therefore, it is possible that adjunctive therapies might have neutralized negative impact of the attenuated plaque on clinical outcome. In our present study, TIMI frame count immediately after initial balloon dilatation was significantly higher in patients with attenuated plaque. However, final TIMI frame count and incidence of final TIMI-3 flow grade were similar between the 2 groups. Possible explanation for the similar final coronary flow status may be the use of adjunctive intracoronary pharmacological treatment and/or additional thrombectomy. Intracoronary administration of nicorandil [9–12], verapamil [11, 12] or nitroprusside [13, 14] has been shown to preserve coronary flow during PCI. In addition, several studies have shown that thrombectomy is effective in patient with AMI [15, 16]. On the other hand, thrombus aspiration may be effective to retrieve plaque gruel after PCI [17]. Kotani et al. [17] reported that more atheromatous plaque, platelet and fibrin complex, macrophages, and cholesterol crystals could be retrieved after PCI from patients with no-reflow as compared with those without no-reflow. Because these adjunctive treatments for slow flow/no reflow were performed based on the each operator's discretion, it is unclear as to which of them were truly effective to improve coronary microcirculation and prognosis. Although additional thrombectomy was performed in all patients with TIMI-0-2 flow during or after PCI, detailed information about the name and the dose of drugs used for adjunctive intracoronary pharmacological treatment is not available. Randomized trials to test the efficacy of intracoronary drug administration or thrombectomy after PCI are needed to answer this question. In addition to the adjunctive intracoronary procedures, statin pre-treatment may also be related to no-reflow in patient with myocardial infarction and better functional recovery [18]. Furthermore, chronic optimal medical therapy, such as antiplatelets, statin, beta-blockers and angiotensin-converting enzyme inhibitors, is known to be related to better long-term clinical outcome. In this study, angiotensin-converting enzyme inhibitors or angiotensin receptor blockers were more frequently used in patients with attenuated plaque. This might have affected the results.

Histological findings of the attenuated plaque have been reported previously [3, 7]. Yamada et al. [7] investigated ex vivo coronary arteries and compared histological findings between attenuated plaque and non-attenuated plaque. Necrotic core and fibrofatty plaque were more frequently detected in attenuated plaque than in non-attenuated plaque. Similarly, in vivo histological examination of directional coronary atherectomy samples showed that attenuated plaque had significantly more atheromatous tissue and less fibrous tissue [3]. More recently, in vivo studies using virtual histology IVUS and OCT demonstrated the similar results [6, 19, 20]. Lee et al. [20] reported that attenuated plaque by IVUS had thinner fibrous cap overlying lipid-rich plaque by OCT. Therefore, it is speculated that